



DE92013242

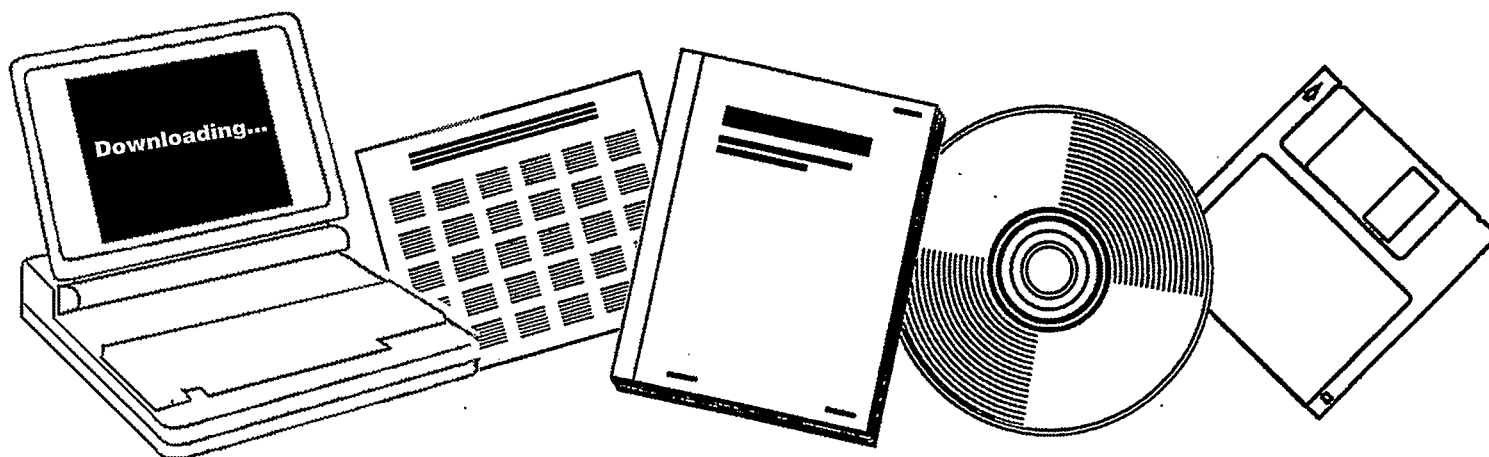
NTIS

One Source. One Search. One Solution.

EFFECT OF CHEMICAL ADDITIVES ON THE SYNTHESIS OF ETHANOL. FINAL TECHNICAL REPORT, SEPTEMBER 15, 1987--MARCH 15, 1992

AKRON UNIV., OH. DEPT. OF CHEMICAL
ENGINEERING

06 MAR 1992



U.S. Department of Commerce
National Technical Information Service

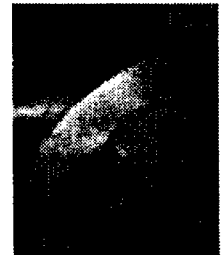
One Source. One Search. One Solution.

NTIS



**Providing Permanent, Easy Access
to U.S. Government Information**

National Technical Information Service is the nation's largest repository and disseminator of government-initiated scientific, technical, engineering, and related business information. The NTIS collection includes almost 3,000,000 information products in a variety of formats: electronic download, online access, CD-ROM, magnetic tape, diskette, multimedia, microfiche and paper.



Search the NTIS Database from 1990 forward

NTIS has upgraded its bibliographic database system and has made all entries since 1990 searchable on **www.ntis.gov**. You now have access to information on more than 600,000 government research information products from this web site.

Link to Full Text Documents at Government Web Sites

Because many Government agencies have their most recent reports available on their own web site, we have added links directly to these reports. When available, you will see a link on the right side of the bibliographic screen.

Download Publications (1997 - Present)

NTIS can now provide the full text of reports as downloadable PDF files. This means that when an agency stops maintaining a report on the web, NTIS will offer a downloadable version. There is a nominal fee for each download for most publications.

For more information visit our website:

www.ntis.gov



U.S. DEPARTMENT OF COMMERCE
Technology Administration
National Technical Information Service
Springfield, VA 22161

THE EFFECT OF CHEMICAL ADDITIVES ON THE SYNTHESIS OF ETHANOL

Final Technical Report

Grant No. DE-FG22-87PC79923

September 15, 1987 - March 15, 1992



Steven S.C. Chuang

Department of Chemical Engineering

The University of Akron

Akron, OH 44325

Date of Submission: March 6, 1992

ABSTRACT

The objective of this research was to investigate the reaction mechanism of higher alcohol and aldehyde synthesis from syngas and the role of additives in the synthesis. An in situ IR reaction system and probe molecule technique were developed to study adsorbed species, active sites, and reaction pathway during reaction. The catalysts used for this study included silica-supported Rh, Ru, and Ni.

IR studies of the reaction of C_2H_4/H_2 with adsorbed CO showed that linear CO adsorbed on the single Rh^0 site and the linear CO adsorbed on the Rh^+ site were consumed and propionaldehyde was produced when adsorbed CO was exposed to C_2H_4 and H_2 . Comparison of the rates of propionaldehyde formation showed that Rh^+ sites were more active than Rh^0 sites. It was concluded that both single Rh^0 atom and Rh^+ ion sites are active for CO insertion. The conclusion was further tested by steady-state ethylene hydroformylation studies. Oxidized Rh/SiO_2 which possesses Rh^+ sites exhibited higher activities for the formation of propionaldehyde than reduced Rh/SiO_2 which mainly contains reduced Rh^0 sites.

Activity of the catalyst for higher alcohol and aldehyde synthesis decreased in the order of $Rh/SiO_2 > Ru/SiO_2 > Ni/SiO_2$. About 50 mol% of acetaldehyde was produced over Rh/SiO_2 at 30 atm and 513 K in CO/H_2 reaction, while Ni/SiO_2 did not exhibit activity for oxygenate

synthesis at this condition. In $C_2H_4/CO/H_2$ reaction, all three catalysts exhibited CO insertion activity leading to the formation of propionaldehyde with selectivity near 20-50 mol%. The main byproducts were methane and ethane in CO/H_2 and $C_2H_4/CO/H_2$ reaction, respectively.

The geometric structure and electronic state of the catalyst surface can be modified by the use of additives. Sulfur additive shifted linear CO band to higher wavenumber, blocked bridge CO sites, and increased the selectivity of catalysts toward oxygenates. Silver tended to produce Rh^+ ions and to block bridge CO sites and led to an enhancement of C_2 oxygenate synthesis on Rh catalysts. The promoter effect of sulfur and silver suggested that highly active and selective catalysts for higher oxygenate synthesis can be obtained by the careful construction of the specific active sites.

TABLE OF CONTENTS

	Page
PUBLICATIONS, PRESENTATIONS, AND THESES	vii
LIST OF TABLES.	xi
LIST OF FIGURES	xii
 CHAPTER	
I. INTRODUCTION	1
1.1 Overview.	1
1.2 Objective	3
1.3 Scope	3
II. LITERATURE REVIEW.	6
2.1 Fischer-Tropsch Reaction.	6
2.2 CO Insertion.	8
2.2.1 CO Insertion in Hydroformylation.	8
2.3 Active Site	10
2.4 Catalysts for High Oxygenate Synthesis.	13
2.5 Effect of Promoters	14
2.6 Reactive Probing.	16
2.7 Sulfur Poisoning.	17
2.8 Infrared Spectroscopy in Catalytic Reactions. . .	21
2.8.1 Infrared Spectroscopy: Theory	21
2.8.2 Application to Catalytic Reaction	24
2.8.2.1 CO Chemisorption.	25
2.8.2.2 Surface Hydrocarbons.	25
2.8.2.3 Surface Oxygenates.	31

III. EXPERIMENTAL	35
3.1 Catalyst Preparation and Characterization	35
3.2 Reactor System.	36
IV. INFRARED STUDY OF THE CO INSERTION REACTION ON REDUCED OXIDIZED, AND SULFIDED Rh/SiO ₂ CATALYSTS	40
4.1 Introduction.	40
4.2 Experimental.	42
4.2.1 Catalyst Preparation and Characterization	42
4.2.2 Experimental Procedure.	42
4.3 Results	43
4.3.1 X-Ray Photoelectron Spectroscopy.	43
4.3.2 CO Adsorption	43
4.3.3 Reaction of Adsorbed CO with C ₂ H ₄ and H ₂	49
4.3.4 Steady State Ethylene Hydroformylation.	55
4.4 Discussion.	63
4.4.1 Characterization of the Rh Surface by Infrared Spectroscopy of CO Adsorption.	63
4.4.2 CO Insertion.	64
4.5 Conclusions	70
V. HIGHER OXYGENATE SYNTHESIS FROM REACTION OF ETHYLENE WITH SYNGAS ON Ni/SiO ₂ AND SULFIDED Ni/SiO ₂	72
5.1 Introduction.	72
5.2 Experimental.	73
5.2.1 Catalyst Preparation and Characterization	73
5.2.2 Experimental Procedure.	73
5.3 Results and Discussion.	74
5.3.1 CO/H ₂ Reaction on Ni/SiO ₂	74
5.3.2 C ₂ H ₄ /CO/H ₂ Reaction on Ni/SiO ₂	77

5.3.3	Sulfur Effect on Ethylene Hydroformylation. .	81
5.4	Conclusions	85
VI.	AN IN SITU INFRARED STUDY OF CO HYDROGENATION AND ETHYLENE HYDROFORMYLATION ON Ru/SiO ₂ AND SULFIDED Ru/SiO ₂	86
6.1	Introduction.	86
6.2	Experimental.	88
6.2.1	Catalyst Preparation and Characterization . .	88
6.2.2	Experimental Procedure.	89
6.3	Results and Discussion.	90
6.3.1	CO Adsorption	90
6.3.2	CO Hydrogenation on Ru/SiO ₂	92
6.3.3	CO Hydrogenation on Sulfided Ru/SiO ₂	96
6.3.4	Ethylene Hydroformylation on Ru/SiO ₂	98
6.3.5	Ethylene Hydroformylation on Sulfided Ru/SiO ₂	102
6.3.6	Dynamic Behavior of Adsorbed Propionaldehyde. .	104
6.3.7	Temperature Programmed Reaction with H ₂ . . .	106
6.3.8	CO Hydrogenation and Ethylene Hydroformylation on the Washed Ru/SiO ₂ . . .	108
6.4	Conclusions	112
VII.	THE EFFECT OF SILVER PROMOTION ON CO HYDROGENATION AND ETHYLENE HYDROFORMYLATION OVER Rh/SiO ₂ CATALYSTS . . .	114
7.1	Introduction.	114
7.2	Experimental.	115
7.2.1	Catalyst Preparation and Characterization . .	115
7.2.2	Experimental Procedure.	116
7.3	Results	116
7.3.1	X-Ray Photoelectron Spectroscopy.	116

7.3.2	CO Adsorption	118
7.3.3	NO Adsorption	118
7.3.4	CO Hydrogenation.	123
7.3.5	Ethylene Hydroformylation	126
7.4	Discussion.	129
7.4.1	Catalyst Characterization	129
7.4.2	Ag Promotion of C ₂ Oxygenate Formation . . .	132
7.5	Conclusions	132
VIII.	THE EFFECT OF CHEMICAL ADDITIVES ON CO HYDROGENATION AND ETHYLENE ADDITION OVER Rh/SiO ₂ CATALYSTS	134
8.1	Introduction	134
8.2	Experimental	135
8.2.1	Catalyst Preparation	135
8.2.2	Experimental Procedure	135
8.3	Results and Discussion	136
IX.	SUMMARY.	146
9.1	Overview.	146
9.2	CO Adsorption	147
9.3	Nature of the Active Site for CO Insertion. . . .	149
9.4	Effect of Silver on C ₂ Oxygenate Synthesis . . .	150
9.5	Oxygenate Synthesis on Ni/SiO ₂ and Ru/SiO ₂	151
9.6	Effects of Aditives	152
9.7	Concluding Remark	152
	BIBLIOGRAPHY.	155
	APPENDICES	164
A.	INFRARED SPECTRA OF GASEOUS HYDROCARBONS	165
B.	INFRARED SPECTRA OF GASEOUS ALCOHOLS AND ALDEHYDES . . .	166

Publications, presentations, and theses resulting from this research grant are listed in the following:

PUBLICATIONS:

1. "Infrared Spectroscopic Studies of Ethylene Hydroformylation on Rh/SiO₂: An Investigation of the Relationships between Homogeneous and Heterogeneous Hydroformylation," J. of Molecular Catalysis, 55, 12-22, 1989. (with S. I. Pien).
2. "Infrared Studies of Reaction of Ethylene with Syngas on Ni/SiO₂," Catalysis Letters, 3,(4), 323-329, 1989. (with S. I. Pien).
3. "C₂ Oxygenate Synthesis from CO Hydrogenation on AgRh/SiO₂," Applied Catalysis, 57, 241-251, 1990. (with S. I. Pien, R. Nayaranan).
4. "Ethylene Addition to CO Hydrogenation over Sulfided Ni, Rh, and Ru," J. of Catalysis, 126, 187-191, 1990 (with S.I. Pien, C. Sze).
5. "Enhancement of Ethylene Hydroformylation over Ni/SiO₂ through Sulfur Promotion," Catalysis Letters, 6, 389-394, 1990 (with S. I. Pien).
6. "Sulfided Group VIII Metals for Hydroformylation," Applied Catalysis, 66, L1-L6, 1990.
7. "Synthesis of Aldehydes from Synthesis Gas over Na-promoted Mn-Ni Catalysts," J. of Catalysis, 128, 569-573, 1991 (with S. I. Pien).
8. "Carbon Monoxide Hydrogenation over Na-Mn-Ni: Effect of Catalyst Preparation Methods on the C₂ Oxygenate Selectivity," Applied Catalysis, 70, 101-114, 1991 (with S. I. Pien, K. Ghosal, Y. Soong, R. P. Noceti, and R. R. Schehl).
9. "The Effect of Adsorbed Sulfur on Heterogeneous Hydroformylation over Rh, Ni, and Ru Catalysts," in Studies in Surface Science and Catalysis Series, Catalyst Deactivation-1991, Eds, C. H. Bartholomews and J. G. Butt, 549-556, Elsevier, Amsterdam-Oxford-New York-Tokyo, 1991 (with M. W. Balakos, S. I. Pien).
10. "The Conversion of Synthesis Gas to Higher Oxygenated Fuel on Rh-based Catalysts: Effects of Chemical Additives," Fuel Science & Technology International, 9(7), 793-810, 1991 (with M. W. Balakos).
11. "An In Situ Infrared Study of Ethylene Hydroformylation and CO Hydrogenation on Ru/SiO₂ and Sulfided Ru/SiO₂," J. of Molecular Catalysis, 68, 313-330, 1991 (with S. I. Pien).
12. "Infrared Study of the CO Insertion Reaction over the Reduced Rh, Oxidized Rh, and Sulfided Rh Catalysts," (with S. I. Pien) J. of Catalysis, in press.

PRESENTATIONS:

1. "The Effect of Additives on the Synthesis of Oxygenated Compounds from CO Hydrogenation and Hydroformylation," 1987 Annual Meeting of AIChE., New York, New York, Nov. 15-20, 1987.
2. "The Effect of Additives on CO-insertion over Rh Catalysts," 27th Symposium of the Pittsburgh-Cleveland Catalysts Society, Cleveland, Ohio, April 6-8, 1988.
3. "The Synthesis of C₂+ Alcohols and Aldehydes over Chemically Modified Rh Catalysts," Invited Talk, Pleasant Valley Laboratory, BP America Inc., Independence, Ohio, April 8, 1988.
4. "The Role of Promoters in the Synthesis of Oxygenated Hydrocarbons," 62nd Colloid and Surface Science Symposium, University Park, PA, June 19-22, 1988.
5. "Infrared Spectroscopic Studies of CO and H₂/CO Adsorption of Supported Rhodium," 28th Annual Symposium of the Pittsburgh-Cleveland Catalysis Society, Pittsburgh, PA, March 29-31, 1989.
6. "The Effect of Sulfur on the Oxygenate Synthesis over Ni and Co Catalysts," 28th Annual Symposium of the Pittsburgh-Cleveland Catalysis Society, Pittsburgh, PA. March 29-31, 1989. (presented by A. Dastidar).
7. "IR Studies of CO/H₂/C₂H₄ Reaction over Ru/SiO₂ and Sulfided Ru/SiO₂," 28th Annual Symposium of the Pittsburgh-Cleveland Catalysis Society, Pittsburgh, PA. March 29-31, 1989. (presented by S. I. Pien).
8. "The Synthesis of C₂+ Oxygenates from CO/H₂ Reaction and CO/H₂/C₂H₄ Reaction on Ag-Rh/SiO₂ Catalysts," 11th North American Meeting of the Catalysis Society, Dearborn, Mich. May 7-11, 1989.
9. "An Infrared Spectroscopic Study of Hydroformylation over Rh/SiO₂ and Sulfided Rh/SiO₂ Catalysts," 11th North American Meeting of the Catalysis Society, Dearborn, Mich. May 7-11, 1989.
10. "The Effect of Chemical Additives on the Synthesis of Ethanol," University Coal Research Conference of Dept. of Energy, Pittsburgh, PA, July 10-13, 1989.
11. "Synthesis of Oxygenates from Syngas Related Reactions," Graduate Seminar, Chemical and Petroleum Engineering Dept. University of Pittsburgh, PA. August 18, 1989.
12. "Infrared Spectroscopic Studies of Ethylene Hydroformylation of Rh/SiO₂: An Investigation of the Relationships between Homogeneous and Heterogeneous Hydroformylation," 6th International Symposium on Relations between Homogeneous and Heterogeneous Catalysis, Pisa, Italy, Sept 25-29, 1989.

13. "Effects of H_2S on the Synthesis of C_2+ Oxygenates from Syngas Reaction on Group VIII Metals," 1989 Annual Meeting of AIChE, San Francisco, California, November 5-10, 1989.
14. "Selective Synthesis of Oxygenates from Syngas Reaction on Mn-Promoted Ni Catalysts," 1989 Annual Meeting of AIChE, San Francisco, California, November 5-10, 1989.
15. "Infrared Spectroscopic Studies of Surface Species during Hydroformylation over Rh/SiO_2 ," 1989 Annual Meeting of AIChE, San Francisco, California, November, 5-10, 1989.
16. "Characterization of Ag-promoted Rh/SiO_2 Catalysts by CO and NO adsorption," 29th Annual Symposium of the Pittsburgh-Cleveland Catalysis Society, Beachwood, Ohio, April 18-20, 1990. (presented by S. I. Pien).
17. "Alkali-promoted Ni-Mn Catalysts for Higher Oxygenate Synthesis," 29th Annual Symposium of the Pittsburgh-Cleveland Catalysis Society, Beachwood, Ohio, April 18-20, 1990. (presented by A. Pant).
18. "Characterization of Rhodium Carbonyl Supported on Silica under Hydroformylation Conditions," 29th Annual Symposium of the Pittsburgh-Cleveland Catalysis Society, Beachwood, Ohio, April 18-20, 1990.
19. "The Effect of Chemical Additives on the Synthesis of Ethanol," Review of Fossil Energy Advanced Research, U.S. Dept. of Energy, Bethesda, Maryland, June 19-20, 1990.
20. "Alkali-promoted Ni and Mo Catalysts for Higher Alcohol Synthesis," 1990 Summer National Meeting of AIChE, San Diego, CA, August 19-22, 1990.
21. "Investigation of the Mechanism of Catalyst Deactivation for CO/H_2 and $CO/H_2/C_2H_4$ on Ni/SiO_2 and $S-Ni/SiO_2$," 1990 Annual Meeting of AIChE, Chicago, IL, November 11-16, 1990.
22. "Investigation of the Mechanism of CO Insertion on the Reduced, Oxidized, and Sulfided Rh/SiO_2 Catalysts," 1990 Annual Meeting of AIChE, Chicago, IL, November 11-16, 1990.
23. "Surface Organometallic Chemistry: Hydroformylation on Silica-supported $Rh^+(CO)_2$ Catalysts," 12th North American Meeting of the Catalysis Society, Lexington, Kentucky. May 5-9, 1991.
24. " H_2 and CO Temperature Programmed Desorption Study of Na-Mn-Ni Catalysts," 12th North American Meeting of the Catalysis Society, Lexington, Kentucky. May 5-9, 1991.
25. "CO Hydrogenation on Bimetallic $Cu-Rh/SiO_2$ and $Ag-Rh/SiO_2$: The Effect of Cu and Ag on the Oxygenate Selectivity," 12th North American Meeting of the Catalysis Society, Lexington, Kentucky. May 5-9, 1991.

26. "Infrared Study of CO and NO Adsorbed on Ag-Rh/SiO₂ Catalysts," 30th Annual Symposium of the Pittsburgh-Cleveland Catalysis Society, Pittsburgh, Pa, May 29-31, 1991. (presented by S. I. Pien).
27. "The Effect of Sulfur on Aldehyde Selectivity in Hydroformylation over Silica-supported Group VIII Metals," 30th Annual Symposium of the Pittsburgh-Cleveland Catalysis Society, Pittsburgh, Pa, May 29-31, 1991.
28. "Ni-based Catalysts for Oxygenate Synthesis: A Temperature Programmed Reaction Study," 30th Annual Symposium of the Pittsburgh-Cleveland Catalysis Society, Pittsburgh, Pa, May 29-31, 1991.
29. "The Effect of Adsorbed Sulfur on Heterogeneous Hydroformylation over Rh, Ni, and Ru Catalysts," 5th International Symposium on Catalyst Deactivation, Chicago, Il, June 23-26, 1991.
30. "Formation and Surface Reactions of Rh⁺(CO)₂/SiO₂," 5th USA-Japan-China Trilateral Symposium on Catalysis, Chicago, Il, June 27-29, 1991.
31. "Higher Alcohol and Aldehyde Synthesis from Syngas over Ni- and Rh-based Catalysts," 1991 Summer National Meeting of AIChE, Pittsburgh, Pa, August 18-21, 1991.
32. "The Effect of Hydrogen Sulfide on the Carbonylation Reactions on Supported Rh metal and Rh carbonyls," 1991 Annual Meeting of AIChE, Los Angeles, CA, November 17-22, 1991.
33. "Characterization and Surface Reactions of Supported Rh Carbonyls and Rh Metal," 1991 Annual Meeting of AIChE, Los Angeles, CA, November 17-22, 1991.

THESES:

1. Pien, S. I., "Higher Oxygenate Synthesis from Syngas over Rhodium, Nickel, and Ruthenium Catalysts," Ph.D. Dissertation, The University of Akron, 1992.
2. Balakos, M. W., "Temperature Programmed Characterization of Ni-based Catalysts for Higher Oxygenate Synthesis," M.S. Thesis, The University of Akron, 1991.
3. Narayanan, R., "The Effect of Silver on Oxygenate Synthesis Using Rhodium Catalyst," M.S. Thesis, The University of Akron, 1989.
4. Sze, C., "The Effect of Sulfur on the Synthesis over Silica Supported Rhodium, Ruthenium, and Nickel," M.S. Thesis, The University of Akron, 1989.

LIST OF TABLES

TABLE	Page
2.1 Nature of Active Sites for Specific Reaction Steps . . .	11
2.2 Effect of promoters and supports	15
2.3 Infrared Spectra of CO Adsorption on Transition Metals .	26
2.4 Infrared Spectroscopy of Hydrocarbon Species	29
2.5 Infrared Spectroscopy of Oxygenate Species	33
4.1 Rates of Products of Ethylene Hydroformylation over Reduced, Oxidized, and Sulfided Rh/SiO ₂ Catalysts. . .	58
5.1 Product Selectivity of CO/H ₂ Reaction on Ni/SiO ₂	76
5.2 Product Selectivity of C ₂ H ₄ /CO/H ₂ Reaction on S-Ni/SiO ₂ and Ni/SiO ₂	79
6.1 CO Hydrogenation over Ru/SiO ₂ and Sulfided Ru/SiO ₂ . . .	94
6.2 CO/H ₂ /C ₂ H ₄ Reaction over Ru/SiO ₂	99
6.3 CO/H ₂ /C ₂ H ₄ Reaction over Sulfided Ru/SiO ₂	103
7.1 Assignment of Infrared Bands for Adsorbed NO	122
7.2 Rates of Product Formation of CO Hydrogenation at 513 K.	125
7.3 Rates of Product Formation of Ethylene Hydroformylation at 513 K	128
7.4 Catalyst Characterization for Various Ag/Rh Ratio. . . .	130

LIST OF FIGURES

FIGURE	Page
2.1 Reaction Mechanism of the Fischer-Tropsch Synthesis. . .	7
2.2 Reaction Pathway of Addition of Ethylene to CO/H ₂	18
3.1 Schematic Diagram of the Experimental Apparatus.	37
3.2 High Pressure IR Cell for in situ IR Studies	38
4.1 Rh 3d _{3/2} , 3d _{5/2} XPS Spectra of Rh/SiO ₂ : (a) after exposure to air at room temperature, (b) after reduction in H ₂ at 513 K for 3 hr, (c) after oxidation in air at 513 K for 3 hr	44
4.2 CO Adsorption on the Reduced Rh/SiO ₂ Catalyst at 301 K .	45
4.3 CO Adsorption on the Oxidized Rh/SiO ₂ Catalyst at 301 K.	47
4.4 Sequential Difference Spectrum of CO Adsorption: obtained from subtraction of spectra in figure 3; spectrum 4a=3b-3a, spectrum 4b= 3c-3b, spectrum 4c= 3d-3c, etc	48
4.5 CO Adsorption on the Sulfided Rh/SiO ₂ Catalyst at 301 K.	50
4.6 Reaction of C ₂ H ₄ /H ₂ with Adsorbed CO on the Reduced Rh/SiO ₂ Catalyst at 301 K.	51
4.7 Reaction of C ₂ H ₄ /H ₂ with Adsorbed CO on the Oxidized Rh/SiO ₂ Catalyst at 301 K.	53
4.8 Sequential Difference Spectrum of the Reaction of C ₂ H ₄ /H ₂ with Adsorbed CO: obtained from subtraction of spectra in figure 7; spectrum 8a= 7b-7a, spectrum 8b= 7c-7b, spectrum 8c= 7d-7c, etc	54
4.9 Reaction of C ₂ H ₄ /H ₂ with Adsorbed CO on the Sulfided Rh/SiO ₂ Catalyst at 301 K.	56
4.10 Ethylene Hydroformylation on the Reduced Rh/SiO ₂	57
4.11 Ethylene Hydroformylation on the Oxidized Rh/SiO ₂	60
4.12 Ethylene Hydroformylation on the Sulfided Rh/SiO ₂	62

5.1	Infrared Spectra of CO/H ₂ Reaction on Ni/SiO ₂ : S.S. (steady state): The spectrum was taken while the reactant flow was maintained at steady state. C.S. (closed system): The spectrum was taken while both the inlet and outlet of IR reactor was closed . .	75
5.2	Infrared Spectra of C ₂ H ₄ /CO/H ₂ Reaction on Ni/SiO ₂ . . .	78
5.3	Infrared Spectra of C ₂ H ₄ /CO/H ₂ Reaction on S-Ni/SiO ₂ . .	83
6.1	Infrared Spectra of CO Adsorption at 513 K: (a) on Ru/SiO ₂ at 10 atm for 20 min, (b) at 1 atm for 20 min, (c) after reduction in flowing H ₂ at a rate of 5 cm ³ /min at 1 atm for 20 min, (d) on S-Ru/SiO ₂ at 10 atm for 20 min, (e) at 1 atm for 20 min.	91
6.2	Infrared Spectra of CO/H ₂ Reaction at 513 K: (A)-(a) on Ru/SiO ₂ at 1 atm, (b) at 10 atm, (c) at 20 atm, (d) at 30 atm, (e) reduction in flowing H ₂ at a rate of 5 cm ³ /min at 1 atm for 20 min; (B)-(a) background: reduction in flowing H ₂ at a rate of 5 cm ³ /min for 10 hr after the CO/H ₂ /C ₂ H ₄ reaction, (b) CO/H ₂ reaction on S-Ru/SiO ₂ at 1 atm, (c) at 10 atm, (d) at 30 atm, (e) reduction in flowing H ₂ at a rate of 5 cm ³ /min at 1 atm of 20 min	93
6.3	Infrared Spectra of CO/H ₂ /C ₂ H ₄ Reaction at 513 K on (A) Ru/SiO ₂ and (B) Sulfided Ru/SiO ₂ : (a) at 1 atm, (b) at 10 atm, (c) at 20 atm, (d) at 30 atm, (e) reduction in flowing H ₂ at a rate of 5 cm ³ /min at 1 atm for 20 min, (f) for 10 hr.	100
6.4	Transient Observation by Switching CO/H ₂ /C ₂ H ₄ Flow to CO/H ₂ Flow at 1 atm, 513 K on (A) Ru/SiO ₂ and (B) Sulfided Ru/SiO ₂ : (a) steady state of CO/H ₂ /C ₂ H ₄ reaction, (b) right after cut off C ₂ H ₄ flow, (c) for 2 min, (d) for 4 min, (e) for 6 min, (f) for 15 min, (g) for 50 min	105
6.5	Temperature Programmed-Desorption of Adsorbed Species with Hydrogen (10 cm ³ /min) on (A) Ru/SiO ₂ and (B) Sulfided Ru/SiO ₂ : (a) at 298 K, (b) at 323 K, (c) at 343 K, (d) at 373 K, (e) at 425 K, (f) at 473 K, (g) at 493 K, (h) at 513 K, (i) at 513 K for 10 hr	107
6.6	Relative Intensity Versus Temperature for the TPR of the Adsorbed CO and Propionaldehyde on Ru/SiO ₂ and Sulfided Ru/SiO ₂ : Relative intensity is the ratio of the intensity of adsorbed species during TPR to the initial intensity of adsorbed species. (□) linear CO on Ru/SiO ₂ , (Δ) propionaldehyde on Ru/SiO ₂ , (□) linear CO on S-Ru/SiO ₂ , (Δ) propionaldehyde on S-Ru/SiO ₂	109

6.7	Infrared Spectra of CO Adsorption, CO/H ₂ , and CO/H ₂ /C ₂ H ₄ Reactions on the Washed Ru/SiO ₂ at 513 K. . .	111
7.1	Rh 3d _{3/2} , 3d _{5/2} XPS Spectra of Rh/SiO ₂ and Ag-Rh/SiO ₂ Catalysts.	117
7.2	Infrared Spectra of CO Adsorption on Rh/SiO ₂ and Ag-Rh/SiO ₂ at 301 K.	119
7.3	Infrared Spectra of NO Adsorption on Silica at 301 K . .	120
7.4	Infrared Spectra of NO Adsorption on Rh/SiO ₂ and Ag-Rh/SiO ₂ at 301 K.	121
7.5	Infrared Spectra of CO Hydrogenation on Rh/SiO ₂ and Ag-Rh/SiO ₂	124
7.6	Infrared Spectra of Ethylene Hydroformylation on Rh/SiO ₂ and Ag-Rh/SiO ₂	127
8.1	Selectivities of products from the reaction of CO/H ₂ at 573 K and 10 atm.	137
8.2	Reaction Pathway for the CO hydrogenation Reaction . . .	139
8.3	Selectivities of Product from the Reaction of CO/H ₂ /C ₂ H ₄ at 573 K and 10 atm.	141
8.4	Reaction Pathway for the ethylene addition reaction. . .	142
8.5	Reaction for the CO Hydrogenation Reaction with the Additives that enhance specific Steps.	144
9.1	Infrared Spectra of CO Adsorption on Reduced and Sulfided Ni/SiO ₂ , Rh/SiO ₂ , and Ru/SiO ₂ at 513 K, 1 atm.	147

CHAPTER I

INTRODUCTION

1.1 Overview

The dwindling supply of non-renewable fossil fuel and the instability of oil prices have stimulated the development of alternative sources of fuel and raw material [1,2]. Agricultural production of biomass may be an attractive alternative [1,3], however, it appears to be inefficient when the cost of cultivation time, dependence of weather, and requirement of large areas of land are taken into consideration.

Syngas, a mixture of carbon monoxide and hydrogen, has been considered as an important feedstock [2]. The syngas can be produced from many carbon sources, especially from coal. The long-term availability of coal makes syngas chemistry especially important. The synthesis of higher oxygenates, especially higher alcohols such as ethanol, from syngas is a viable and attractive route for the production of clean fuel as well as a potential feedstock in the production of organic chemicals presently derived from crude oil [3,4].

The processes for the direct synthesis of higher alcohols from syngas include modified methanol synthesis and the Fischer-Tropsch (F-T) synthesis. Modified methanol synthesis catalysts such as Cs/Cu/ZnO-based catalysts and Co/Cu/Zn/Al₂O₃ catalysts have been

demonstrated to produce high yields of methanol and higher alcohols 2
[5-7]. However, these catalysts require use of high pressure (at least 50 atm) and the catalysts are not highly resistant to sulfur poisoning. In the F-T synthesis, the direct conversion of syngas may yield a broad product spectrum of paraffins, olefins, and oxygenates [8]. The product distribution strongly depends on catalyst compositions and reaction conditions. Due to the polymerization nature of the reaction, only C₁ products, CH₄ and CH₃OH, can be produced with 100% selectivity. Tailoring the catalyst surface for the selective synthesis of higher hydrocarbons and oxygenates remains a challenging goal in F-T technology. It has been found that Rh catalysts are highly selective and active for C₂ oxygenate synthesis; increasing evidence has shown that the activity and selectivity of the catalyst for C₂ oxygenates synthesis can be greatly enhanced by the use of additives or supports [9-12]. A better understanding of the role of additives and supports in the F-T process is essential to further improvement of the activity and selectivity of Rh catalyst for C₂ oxygenate synthesis.

Spectroscopic techniques have improved the capability of exploring catalytic reactions. Infrared spectroscopy is one of the spectroscopy techniques that can be used to study catalytic surface reaction under higher pressure and temperature conditions [13,14]. Infrared spectroscopy of CO adsorption has been well established to characterize the surface state of catalysts. Changes in both the frequencies and intensities of the infrared bands of adsorbed species can be used to elucidate the nature and environment of the catalyst surface [15-17].

1.2 Objective

The major problems associated with the synthesis of higher oxygenates from the F-T reaction over Group VIII metal catalysts are low selectivity for higher oxygenates and high selectivity for hydrocarbon products. The solution to these problems lies in our understanding of the reaction mechanism of higher oxygenate synthesis and in our ability to prepare a catalyst that is specifically selective for higher oxygenate synthesis. Extensive mechanistic study of higher oxygenate synthesis has shown that the CO insertion step is a key step for the formation of higher oxygenates. However, the sites for CO insertion remained unclear. Thus, the prime objective of this research was to develop a better understanding of heterogeneously catalyzed CO insertion and the role of additives in the higher oxygenate synthesis. Understanding the active site for CO insertion and the role of chemical additives in CO insertion should enable us to design highly active and selective catalysts for the production of higher alcohols.

1.3 Scope

The uniqueness of this research is to develop an in situ infrared (IR) technique to study higher oxygenate synthesis and characterize the catalysts under practical reaction conditions (1-60 atm, 303-513 K). The catalysts used for this study included silica-supported rhodium, ruthenium, and nickel catalysts. Rh-based catalysts have been extensively studied for F-T activity because of their high C₂ oxygenate selectivity. Ni/SiO₂ (a methanation catalyst) and Ru/SiO₂ (a higher hydrocarbon synthesis catalyst) have been known as F-T catalysts for hydrocarbon synthesis. The effort was aimed at shifting their hydrocarbon selectivity to higher oxygenate selectivity.

The research was conducted in the following areas.

4

- (i) CO adsorption: CO adsorption on the catalyst surface was examined by IR. Because the vibrational frequency of adsorbed CO is very sensitive to the structure and oxidation state of the metal surface, adsorbed CO can serve as an excellent probe to characterize the state of the metal surface before, during, and after the reaction.
- (ii) Reactive probing: Reactive probing by the addition of ethylene into the reaction stream of CO and H₂ permits elucidation of the reaction pathway and identification of the active site for CO insertion.
- (iii) CO hydrogenation and ethylene Hydroformylation: In situ IR coupled with on line GC was used to detect the reactive intermediates and the product distribution.
- (iv) Promoter effect: The experiment was designed to study the promoter effect on Rh catalysts. Silver was selected as the promoter because of its electronegativity was close to that of the Rh atom. The influence of Ag was examined by adding an increasing amount of Ag and by measuring catalytic activity and selectivity as well as chemisorption of probe molecules as a function of Ag content.
- (v) Selective sulfur poisoning: Sulfur is known for its high electronegativity and has been shown to suppress the activity of CO hydrogenation and influence the selectivity of F-T synthesis. The selective sulfur poisoning technique was used to enhance CO insertion activity and selectivity of the Rh and Ni catalysts.

The results of these studies should provide the information 5
of the reaction pathway, the surface state of the catalyst, the
interaction between chemical additives and the active metal, which can
be used to design highly active and selective catalyst surface for C₂
oxygenate synthesis.

CHAPTER II

LITERATURE REVIEW

2.1 Fischer-Tropsch Reaction

Fischer-Tropsch (F-T) reaction is a reaction of carbon monoxide with hydrogen. The reaction yields paraffins, olefins, and oxygenated products such as alcohols, aldehydes, and acids. The mechanism of the F-T reaction has been extensively studied [18-22]. The formation of hydrocarbons and oxygenates from syngas has been demonstrated to occur via the reaction scheme outlined in Figure 2.1.

- (1) dissociation of CO on the catalyst surface forming surface carbon [23-37].
- (2) hydrogenation of the resulting carbon producing CH_2 and CH_3 species as CH_x hydrocarbon intermediates [23-37].
- (3) hydrogenation of the CH_3 species forming hydrocarbons or CH_2 insertion inducing longer alkyl groups [32-37].
- (4) insertion of CO into the alkyl-metal bond leading to the formation of C_2 , oxygenates [36-44].

The above mechanism shows that the competitive reactions, i.e., hydrogenation of CH_x , insertion of CH_2 into CH_x , and CO insertion into CH_x results in a broad product distribution. Enhancement of CO insertion and suppression of hydrogenation have been an important research subject in syngas chemistry.

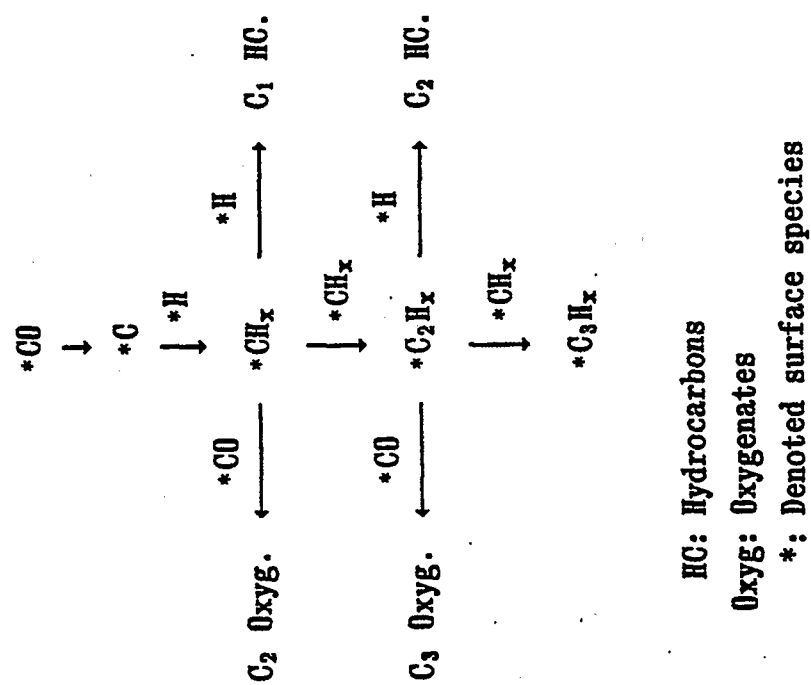
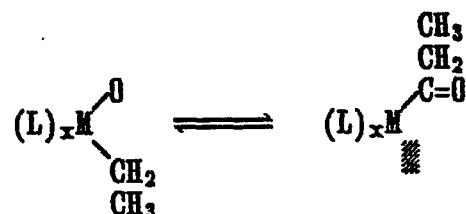


Figure 2.1 Reaction Mechanism of the Fisher-Tropsch Synthesis

The mechanism of CO insertion into a carbon-metal σ bond has been well developed in organometallic chemistry [45-47]. The reaction involves a migration of an alkyl group to the carbon of the CO ligand on the metal center as shown in the following equation:

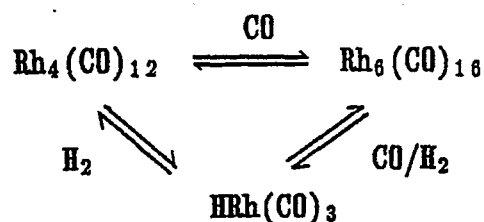


The vacant coordination site (---) resulting from the migration can be filled by an incoming ligand (L) which in many cases is CO.

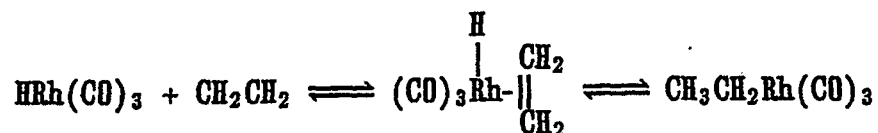
2.2.1 CO Insertion in Hydroformylation

One of the important reactions involving CO insertion in organometallic chemistry is hydroformylation reaction catalyzed by group VIII transition-metal carbonyls [47-52]. Hydroformylation is a reaction of olefin with carbon monoxide and hydrogen. The primary product of hydroformylation is aldehyde containing one more carbon atom than the olefin substrate. More than 90% selectivity of propionaldehyde has been obtained in ethylene hydroformylation reaction [52,53]. The mechanism of ethylene hydroformylation catalyzed by the rhodium-carbonyl complex has been shown as following:

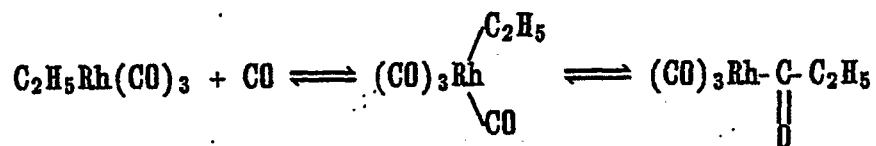
- (1) Activation of catalyst by conversion of parent carbonyl such as $\text{Rh}_4(\text{CO})_{12}$ and $\text{Rh}_6(\text{CO})_{18}$ into hydridocarbonyl, $\text{HRh}(\text{CO})_3$, depend on the condition.



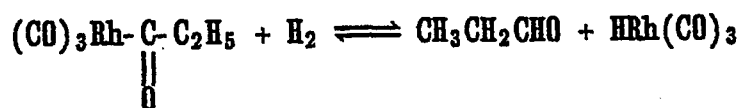
- (2) Insertion of ethylene into a metal-H bond of the hydridocarbonyl to form an alkylmetal complex.



- (3) Migratory insertion of CO into the alkyl-metal bond of the alkylmetal complex to form an acyl species.



- (4) Hydrogenolysis of acyl species to form an aldehyde with regeneration of the catalyst.



Ethylene hydroformylation is known as a homogeneous reaction. The migratory CO insertion occurs on a monoatom center with an oxidation state of +1 [46-50]. Recently, an increasing evidence has shown that ethylene hydroformylation is also catalyzed by supported-metal catalysts, i.e., a heterogeneous reaction [54,55]. Although the migratory CO insertion mechanism in homogeneous hydroformylation has been used to explain the formation of propionaldehyde in reaction of

ethylene with CO and H₂ as well as the formation of C₂ oxygenates in syngas reaction over supported transition metals [56-61], the nature of active sites for CO insertion on supported-metal catalysts are still unclear.

10

2.3 Active Site

Table 2.1 summarizes the proposed active sites for the specific reaction steps in CO hydrogenation (F-T reaction). It is generally agreed that CO dissociation, hydrogenation, and chain growth take place on metal sites [62,63]. However, the nature of the active sites in C₂ oxygenate synthesis is not well understood. Both Rh⁺ and Rh⁰ sites have been proposed to be active for C₂ oxygenate synthesis:

(a) Evidence of Rh⁺ as the active sites:

- (i) In analogy with homogeneous catalysis, the reaction occurring on the metal complex may take place on the metal surface. Since the oxidation state of metal center in metal complex maintain +1 during CO insertion, it has been suggested that the Rh⁺ on the surface of supported Rh can also serve as the active site for CO insertion [58].
- (ii) Results of an ESR study [64] on a Mn-promoted Rh/SiO₂ catalyst indicated that Mn formed a Mn-O-Rh surface compound. Reaction results further suggested that enhanced C₂ oxygenate selectivity under syngas reaction conditions was due to stabilization of an Rh oxide on the metal surface by the mixed oxide formation.
- (iii) CO hydrogenation over hydrated and anhydrous rhodium oxides showed that the hydrated rhodium oxide was active for oxygenate synthesis, while the anhydrous rhodium oxide only exhibited moderate methanation activity. Studies of AES and XPS on these

Table 2.1 Nature of Active Sites for Specific Reaction Steps

Specific Reactions	Oxidation State	Geometric Requirements
$\text{CO} \longrightarrow \text{C} + \text{O}$	metal	ensemble [19,20,62]
$\text{C} + \text{X H} \longrightarrow \text{CH}_x$	metal	a small number of metal surface atoms [22,63]
$\text{CH}_x + \text{CH}_x \longrightarrow \text{C}_2\text{H}_y$	metal	ensemble [19,22]
$\text{CH}_x + \text{CO} \longrightarrow \text{C}_2 \text{ Oxyg. (CO insertion)}$	metal, metal ion, in controversy	a single atom [30,39-41]

rhodium oxide after treatments identical to the reaction conditions found that the hydrated rhodium oxide was quite stable, while the anhydrous oxide rapidly reduced to metallic rhodium under the reaction conditions [58,59].

- (iv) XPS measurement of oxide-supported catalyst showed that (1) Rh on SiO_2 , active for hydrocarbon formation, showed an electronic state similar to Rh metal; (2) Rh and ZnO , active for methanol formation, was in a state close to Rh(I) ; and (3) Rh on ZrO_2 and $\text{TiO}_2/\text{SiO}_2$ was active for C_2 oxygenate formation and showed an oxidation state between that on ZnO and SiO_2 [65].

(b) Evidence of Rh^0 as the active sites:

- (i) Van der Lee et al. [66] reported that V_2O_3 , La_2O_3 , Mg(OH)_2 , and MgO supported Rh catalysts have different activity for methanol and C_2 oxygenate synthesis. An atomic adsorption spectroscopy of the extracted ionic Rh from these catalysts indicated that presence of Rh ions was essential for methanol synthesis, however, Rh ion was not the site for C_2 oxygenate synthesis. They concluded that activity in C_2 oxygenate synthesis was related to metal surface modified by the supports. Similar conclusion was also reported by Katzer et al. that the oxide-supported Rh was in metal-like state as interacted with SiO_2 , Al_2O_3 , CeO_2 , TiO_2 , and MgO supported Rh catalysts [67].
- (ii) Gysling et al. found no evidence for the existence of Rh^+ on the LaRhO_3 catalyst which is active for the synthesis of C_2 oxygenates [68]. They concluded that CO insertion took place on the Rh^0 site instead of the Rh^+ site.

Most data on oxidation states of the catalysts were obtained 13
by XPS studies. The use of XPS is restricted for the measurement before and after the reaction and it might result in the controversial argument of the nature of the active site. Development of an efficient method to directly detect the surface state of the catalyst under reaction condition will help clarify the controversy.

2.4 Catalysts for High Oxygenate Synthesis

The mechanism of the F-T reaction as shown in Figure 2.1 indicates that the direct synthesis of C_2 oxygenates involves CO insertion into the CH_3 intermediate which is produced from dissociatively adsorbed CO. Accordingly, catalysts with both dissociatively adsorbed CO and associatively adsorbed CO may be active for producing C_2 oxygenates.

The capability of group VIII metals in CO dissociation has been well established [69,70]. Co, Ni, Ru, and Fe metals which easily dissociate CO have been known as F-T catalysts and produce mainly hydrocarbons and minor amount of oxygenates [8,71]. Pt, Ir, and Pd metals, which show low CO dissociation activity have excellent catalytic activity for methanol synthesis [72]. However, the Pt, Ir, and Pd are not active for C_2 oxygenate synthesis which may be due to the low CO dissociation activity. Favre et al. [73], working with V_2O_5 -supported Pd, showed that C_2 oxygenates can be produced after supplying the CH_x units, such as CH_2Cl_2 , to the CO/ H_2 mixture.

Rh has been known to exhibit the best selectivity to C_2 oxygenate synthesis. In homogeneous hydroformylation catalyzed, the activity of group VIII transition-metal complexes in CO insertion decreases in the order of $Rh \gg Co > Ru > Fe > Ni$. [47,49,51].

Moreover, the selectivity for CO insertion into adsorbed ethylene over supported metal in the order of Rh >> Ni > Ru > Pd has been reported [57,74]. The unique catalytic ability of Rh may be due to its moderate activity in CO dissociation as well as its high CO insertion activity. 14

2.5 Effect of Promoters

Promoters are additives which improve the activity, selectivity, or stability of unpromoted catalysts [75]. Recent work has found that the support may also act as a promoter and affect the performance of the active metal [76]. Table 2.2 lists the effects of promoters and supports on syngas reaction over Rh-based catalysts. Addition of promoter on Rh-based catalysts leads to various selectivity toward oxygenated products: (i) Methanol is enhanced by ZnO, CaO, and MgO oxides [44,77]; (ii) C₂ oxygenates is produced when Zr, Ti, V, and La oxides are used as promoters or supports [38,78]; and (iii) higher selectivity of oxygenates were obtained by alkali-promoted catalysts [79-83]. However, hydrocarbons are dominated products on silica and alumina supports [60].

The effects of promoters and supports on catalysts can generally include (i) blockage of surface sites of the catalysts, (ii) modification of the catalysts by the chemical effect of the additives, and (iii) activation and stabilization of surface species.

Zn-promoted Rh/SiO₂ catalysts showed that the Zn increased the ethylene hydroformylation activity, decreased ethylene hydrogenation activity and completely suppressed the formation of methane [83]. This observation suggested that Zn blocked sites for CO dissociation. Infrared spectra for these samples showed that increases in Zn content

Table 2.2 Effect of promoters and supports

Catalyst	Additives	Additive effects	Ref.
Rh/SiO ₂	Mn, Mo	High yields of ethanol and higher alcohol with up to eight carbon atoms were achieved.	40
Rh/SiO ₂	Mn	Significantly enhanced the CO conversion rate. Remained high selectivity for C ₂ oxygenates.	64
Rh/SiO ₂	Fe	Did not influence the CO conversion. Changed the products from CH ₃ CHO and CH ₃ COOH to EtOH and MeOH.	60
Rh/SiO ₂	Zn	Decreased chemisorption of CO and H ₂ . Depressed reactive desorption of CO to form methane.	84
Rh/SiO ₂	Mn, Ti, Zr	Lowered the temperature of CO ₂ formation due to the Boudouard reaction. $2\text{CO} \longrightarrow \text{C} + \text{CO}_2$	30
Rh/SiO ₂	Ti, Zr	Enhanced CO dissociation. Lowered the temperature of methane formation due to hydrogenation of CO	78
Rh/TiO ₂	Alkali	Hydrogenation ability decreased in the order of none > Li > K > Cs. K and Cs Suppressed ethylene incorporation into higher hydrocarbon.	81
Rh/TiO ₂	Alkali	Suppressed hydrogenation activity. Selectivity for oxygenated products decreased in the order of Cs = K > Li > none. Overall activity decreased in the order of none > Li > K > Cs.	80
Rh/SiO ₂	K	Increased rate constants for CO dissociation and for hydrogenation of surface carbon species when K/Rh < 0.02. Decrease both rate constants when 0.02 < K/Rh < 0.1.	88
Rh	ZnO, MgO	Predominantly formed methanol.	60
	Al ₂ O ₃ , SiO ₂	Hydrocarbons prevailed in the reaction production.	
Rh	ZrO ₂ , TiO ₂ La ₂ O ₃	Were effective for the formation of ethanol.	10
Rh	ZrO ₂ , Nb ₂ O ₅ TiO ₂	Significantly enhanced the CO conversion rate. Produced ethanol with selectivity of 95% of the oxygenated compounds.	12

suppressed bridged CO more than linear CO [83,84]. The dramatic change in the ratio of bridged and linear CO is similar to the observation of Ag- and Fe-promoted Rh/SiO₂ [85,86].

Modification of the catalyst properties by chemical effect has been observed upon the addition of alkali promoters to metal resulting in enhancement of adsorption energy and dissociation of CO and suppression of catalyst activity of hydrogenation [82,87,88]. A strong metal-support interaction (SMSI) may occur when oxide supports such as TiO₂ and V₂O₃ are used [89,90].

Activation and stabilization of oxygenated compound have been suggested to change CO dissociation activity and oxygenate selectivity. Highly oxophilic ions, such as Mn, Ti, Zr, and Nb, tend to interact with the oxygen atom of the CO adsorbed on the metal [83]. Basic ions such as Fe⁺ on Rh-Fe carbonyl cluster derived catalyst was proposed to stabilize surface oxygenated compound by coordinated oxygen with Fe⁺ [91]. Addition of Mn and Mo compounds on silica-supported Rh formed mixed oxides which stabilize positive Rh ions [64,92]. Infrared spectra also shows that the presence of additives promoted formation of certain reaction intermediates: the acetate and acetyl species over Na-Rh/SiO₂, Mn-Rh/SiO₂, Mn-Li-Rh/SiO₂ and La-Rh/SiO₂ catalysts were detected [10,38,93].

2.6 Reactive Probing

The addition of probe molecules, especially the low molecular weight olefins, has been widely used for studying the complex F-T reaction mechanism [58,74,94]. It has been observed a carbonylation of C₂H₄ to C₂H₅CHO by addition of ethylene to a reaction mixture of CO and H₂ over rhodium catalysts. The C₂H₄ addition results in the

enhancement of propionaldehyde leading to elucidation of the role of CO insertion in C_2 oxygenate synthesis. Chuang and coworker [55,81,82] has been applied ethylene as the probe molecules in CO hydrogenation over silica-supported Rh, Ru, Ni, and Pd catalysts. The study showed that the addition of ethylene to CO/ H_2 resulted in a significant variation in the rate of the formation of certain products and clearly determined the activities of different catalysts for hydrogenation, CO insertion, incorporation, and hydrogenolysis. Jordan and Bell [95] used ^{13}C -labeled CO and H_2 over the Ru/ SiO_2 catalyst to elucidate the effect of ethylene in CO hydrogenation and the differentiate carbon sources.

A possible reaction pathway for the addition of ethylene to CO and H_2 is shown in Figure 2.2. The addition of ethylene during CO hydrogenation could produce adsorbed ethyl species which may undergo (i) hydrogenation to form ethane, (ii) CO insertion to form acyl species which can be hydrogenated to propionaldehyde, (iii) chain incorporation to form higher hydrocarbons, and (iv) hydrogenolysis to form methane. The use of ethylene as a reactive probing molecule provides an effective way for studying the reaction steps involved in higher oxygenate synthesis.

2.7 Sulfur Poisoning

Sulfur compound has been known as a sever poison for a large number of catalytic reactions [96-98]. The dissociation of sulfur compound, such as H_2S , CS_2 , and SO_x having unshared electron pairs, leads to adsorbed sulfur atom strongly bonded to the metal. The change in the work function from the adsorption of sulfur on single-crystal

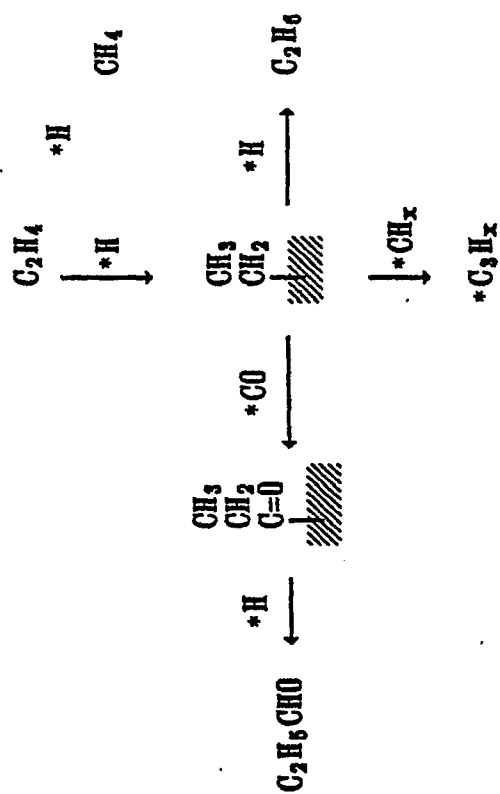


Figure 2.2 Reaction Pathway of Addition of Ethylene to CO/H₂

planes of clear metals has suggested that the bonding of the adsorbed sulfur to Ru and Ni are essential covalent [99,100].

A linear correlation between the decrease in capacity of H_2 adsorption and the surface coverage of sulfur over silica- and alumina-supported Ni indicated that poisoning of Ni atoms varied with the concentration of surface sulfur; the molar ratio of H_2S molecule and surface Ni atom varied from 1/3 to 3/4 was reported [101-103]. Studies of single-crystal Ni [104-106] showed that the decrease in H_2 adsorption is not linear over the full range of sulfur coverage. At low coverage ($\theta_s < 0.2$), a linear decrease in the sticking coefficient showed poisoning of about four Ni atoms per adsorbed sulfur atom. Both studies on supported and single-crystal Ni suggested that electronic effect may be important at low coverage since one atom of sulfur can prevent hydrogen adsorption on three or more Ni atoms. At complete coverage, a simple blocking or geometric effect is adequate to explain the poisoning since the ensembles of Ni for dissociation of H_2 are no longer accessible at the surface. Similarly, presence of sulfur decreased adsorption capability of H_2 and the binding energy of hydrogen on Ru and Pt as indicated by the reduce of the intensity of H_2 adsorption peaks and the shift of the peaks to lower temperature [97]. Sulfur blocks four Ru atoms on single-crystal Ru(100) also reported [107].

The effect of sulfur on CO adsorption is more complex than that on H_2 adsorption. Studies on CO adsorption over Ru(001) single-crystal showed that the sticking coefficient and binding energy of CO are constant up to a total coverage of CO and sulfur corresponding to one adsorbate molecule or atom per three metal atoms. Beyond this

concentration an abrupt decrease in binding energy for CO is observed [108]. Significant sulfur effect on CO adsorption over Ni has been observed. On supported Ni catalysts, presence of sulfur promotes the formation of nickel carbonyl, Ni(CO)_2 or Ni(CO)_4 , leading increases in the capacity of CO adsorption at 190-298 K and pressure above 0.1 KPa [109]. However, sulfur reduces CO adsorption on single-crystal Ni at low CO pressure (less than 0.5 KPa) [110].

Little effort has been put on the coadsorption studies between sulfur, H_2 , and CO over Rh catalysts. Jackson et al. [111] studying the effect of H_2S on the adsorption of CO on silica-supported RhCl_3 and Rh_2O_3 found that CO still adsorbed on the surface with saturated sulfur. On the Rh_2O_3 catalyst carbon monoxide could displace adsorbed hydrogen sulfide. Konishi et al. [112] found that initial increase in surface coverage of sulfur decreased CO adsorption; further dosage of sulfur did not affect CO adsorption when the chemisorption of CO fall to one-third of the original amount on the clean rhodium.

IR data have shown that presence of sulfur on Rh, Ru, and Ni catalysts suppresses bridging bonded CO and shifts the vibrational frequency of the linearly adsorbed CO to a higher wavenumber [112-114], indication that sulfur alters the adsorption of CO by blockage of the active surface sites (geometric effect) and by interaction of metal-sulfur (electron effect).

The modification of the adsorption of reactant molecules such as CO and H_2 by sulfur leads to a partial or complete loss of activity for many reactions steps in syngas reaction. Early investigations have been shown that sulfur has less poisoning effect on oxygenate synthesis than on hydrocarbon synthesis [55,74]. The addition of sulfur

compounds on the catalyst should inhibit the formation of methane and other CO hydrogenation products in the reaction of ethylene addition and ethylene hydroformylation.

2.8 Infrared Spectroscopy in Catalytic Reactions

2.8.1 Infrared Spectroscopy: Theory

Infrared spectroscopy is an adsorption spectroscopy of electromagnetic radiations. The electromagnetic radiation can be characterized by the wavenumber (cm^{-1}), which is defined as the reciprocal of the wavelength. The energy of the infrared radiation is proportional to its wavenumber and extends in the region from 4000 cm^{-1} to 200 cm^{-1} . The infrared spectra arise from adsorption of electromagnetic radiation at discrete frequencies corresponding to quantum modes of vibration and/or rotation of molecular or surface groups.

The Schrodinger equation describes the radiation in wave equation.

$$\nabla^2 \psi + \frac{2m}{\hbar^2} [E - V] \psi = 0$$

For the simple harmonic vibration, Hook's law provides the potential energy as

$$V = \frac{1}{2} k r^2$$

Solution of the Schrodinger equation gives the vibrational energy with

$$E_{\text{vib}} = h c \nu (v + 1/2)$$

where ν is the frequency of vibration (in cm^{-1}) of the oscillator and v is the vibrational quantum number. The energy between quantized levels, according to the selection rule of $\Delta v = \pm 1$, is equivalent to the

energy of an infrared photon whose frequency is ν , i.e.,

$$\Delta E_{\text{vib}} = h\nu$$

Because the vibration of real molecule are anharmonic, the vibration energy becomes

$$E_{\text{vib}} = h\nu[(\nu + 1/2) - \eta(\nu + 1/2)^2 + \dots]$$

where η is the anharmonic constant. The values of η vary from 0.01 to 0.05 for single bonds [105]. Because of the anharmonicity, the vibrational variation of $\pm 1, \pm 2, \dots$ are allowed. The vibrational spectrum may therefore contain the fundamental ($\nu=0 \rightarrow \nu=1$) vibrational band as well as overtones ($\nu=0 \rightarrow \nu=2,3,4,\text{etc.}$) [105,106].

A quantum mechanical treatment of rotational motion can be given by

$$E_{\text{rot}} = \frac{h^2}{8\pi^2 I} J(J+1) = BhcJ(J+1)$$

where I is the moment of inertia; B is the rotational constant; and J is the rotational quantum number which can be the values 0,1,2,etc. Rotational transitions are generally restricted to $\Delta J=1$. The transition $J \rightarrow J+1$ results in the adsorption of infrared radiation which is the same as the increase in rotational energy of the molecule. i.e., $\Delta E_{\text{rot}} = 2Bhc(J+1)$

The rotational frequency of the simple rigid rotator is a function of the rotational quantum number.

In practical infrared spectrum the rotation of a molecule creates a centrifugal force that couples with the vibration, and the result spectral adsorption is due to the combined vibration-rotation, i.e., $E_{\text{v+r}} = h\nu(\nu + 1/2) + BhcJ(J+1)$

A polyatomic linear molecule can have two types of vibrational- rotational bands: a parallel band and perpendicular band depending on the change in dipole moment is parallel or perpendicular to the molecular axis. For the parallel band the selection rule is $\Delta J = \pm 1$. For the perpendicular band the selection rule is $\Delta J = 0, \pm 1$.

Let J and J' represent the rotational quantum number in the ground state and first excited state, respectively.

When $\Delta J = 0$ and $J' = J$,

$$\Delta E_{v+b}/hc = \nu = Q(\text{cm}^{-1})$$

This equation independent of the value of J gives the frequency in Q branch of the band.

When $\Delta J = 1$ and $J' = J+1$,

$$\Delta E_{v+b}/hc = \nu + 2B(J+1) = R(\text{cm}^{-1}) \quad J = 0, 1, 2, \dots$$

This equation gives the frequencies of the rotational lines which make up the R branch.

When $\Delta J = -1$ and $J' = J-1$,

$$\Delta E_{v+b}/hc = \nu - 2B(J) = P(\text{cm}^{-1}) \quad J = 1, 2, 3, \dots$$

The rotational quantum of the P branch cannot be zero since J' is one integer lower than J [115].

In addition to the selection rule in quantum number, a vibration frequency is IR-active only if the change in the magnitude of the dipole moment takes place [115,116]. The dipole moment is defined as the charge time the distance to mass center. Hence, the symmetric vibration of a symmetrical molecule is IR-inactive; its vibration does not appear in the infrared spectrum.

The emerging intensity (I) of the radiation after impinging infrared radiation with intensity I_0 on the substance of thickness d is

giving by the equation [117]

$$I = I_0 e^{-\epsilon d}$$

The quantity ϵ is the extinction coefficient and the product ϵd is the optical density which describe the adsorption characteristics of the material at any given wavenumber. A plot of optical density against wavenumber gives the adsorption spectrum. In practical application, the infrared spectrum is represented by transmittance (T) and absorbance (A) which are defined as

$$T = I/I_0 = e^{-\epsilon d}$$

and $A = \ln(1/T) = \epsilon d$

According to Beer's law, the absorbance is a linear function of concentration for solution and gases. The absorbance is given by

$$A = \epsilon cd$$

where ϵ becomes the molar extinction coefficient; d is the path length; and c is the concentration. Integral of the absorbance of the spectrum is proportional to the concentration. The concentration can be obtained provided that the extinction coefficient is known.

2.8.2 Application to Catalytic Reaction

Infrared spectroscopy has been extensively used as a probe to adsorbed species. The distinct advantages of infrared (IR) spectroscopy are that:

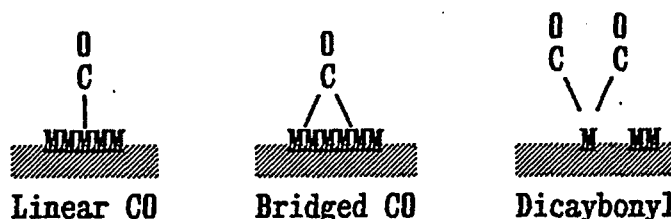
- (i) IR spectra of adsorbed species under high pressure and high temperature conditions can be obtained by use of high pressure and temperature IR cell.
- (ii) IR is of high sensitivity of stretching frequency to bonding modes at surfaces and is able to characterize small shifts in vibrational frequency of the adsorbed species.

(iii) Strong correlation of the spectra of surface species with spectroscopy of molecules of known structure has been established.

In situ IR is a powerful technique for studying higher oxygenate synthesis because the reactant (CO), reaction intermediates, and product molecules exhibit vibrational frequencies in the infrared range.

2.8.2.1 CO Chemisorption

The adsorbed CO on the surface of Group VIII metals has been characterized as linear CO attached by one end to one metal atom; bridged CO attached to two or more atoms; and multi-carbonyl associated



with CO on an isolated metal atom [118-125]. Table 2.3 lists the vibration frequencies of adsorbed CO on transition metal catalysts. Differences can be seen between spectra of CO adsorbed on different transition metals on the same support after similar reduction procedures [121-131]. The presence of promoters shifts the wavenumber and changes the intensity of the CO adsorption band [36,88,89,132]. Such differences usually reflect differences in the geometric structure and oxidation state of the catalyst surface.

2.8.2.2 Surface Hydrocarbons

Table 2.4 lists the vibrational frequencies of hydrocarbon species over supported transition metals [133-139]. The vibration modes of adsorbed hydrocarbon species in infrared spectrum represent in

Table 2.3 Infrared Spectra of CO Adsorption on Transition Metals

Catalyst/ Adsorption Condition	Preparation	Wavenumber (cm ⁻¹)	Assignment/Observation	Reference
Rh/Al ₂ O ₃ 300 K 50 Torr	Precursor: RhCl ₃ R _t : 450 K ⁷	2055 (10 wt% Rh) 2063 (2.2 wt% Rh) 1900 (10 wt% Rh) 1850 (2.2 wt% Rh)	(L) ^a linear and bridged CO bands were not observed over (B) ^a 0.2 wt% Rh, with highly dispersed Rh metal	(121) Cavangh Yates
		(sym) (asym) 2130, 2030 (10 wt% Rh) (DI) ^a 2103, 2030 (2.2 wt% Rh) 2096, 2025 (0.2 wt% Rh)		
Rh/Al ₂ O ₃ 473 K 4.5 Torr	Precursor: (n-Butyl) ₄ Rh ₂ (CO) ₂ Br ₂ R _t : 673 K	(sym) (asym) 2090, 2020 (2050 cm ⁻¹) and bridged CO bands (1850 cm ⁻¹) were developed and dicarbonyl species were diminished		(126) Dietor Roberts
		2072 (R _t : 1173 K) (L)		(16) Solymosi Passtor
Rh/Al ₂ O ₃ (1 wt%) 300 K 50 Torr	Precursor: RhCl ₃ O _t : 573 K ⁷ R _t : 573-1273 K	(sym) (asym) 2010, 2030 (R _t : 573 K) (DI) 2010, 2030 (R _t : 1173 K)	more intensive dicarbonyl bands were observed with R _t = 1173 K	
		2040-2050 2112-2205 1898-1920 (sym) (asym) 2098, 2040	(L) Rh ⁰ (CO) ₂ ^β Rh ⁺ (CO) ₂ ^β Rh ₂ ⁰ (CO) (DI) Rh(CO) ₂	(17) Li Gonzalez

a: (L): linear CO, (B): bridged CO, (DI): dicarbonyl.

β: o: metal with reduced state, +: metal with oxidation state of +1.

7: R_t: reduction temperature, O_t: calcination temperature.

Rh/Al ₂ O ₃ (2.2 wt%) 300 K 6 Torr	Precursor: RhCl ₃ R _t : 423-673 K	2008 (R _t : 423 K) 2066 (R _t : 493 K) 2076 (R _t : 573 K) 2088 (R _t : 673 K)	(L)	CO adsorption on 0.5 wt% Rh for all reduction Temp. showed that: dicarbonyl were observed at 2097-2095 (sym) and 2029-2022 (asym) and linear and bridged CO were not observed	(123) Rice Vorley Curtis Guin Tarrer
		(sym) (asym) 2096, 2024 (R _t : 423 K) (DI) 2100, 2027 (R _t : 493 K) 2098, 2026 (R _t : 573 K)	(DI)		
		2063 (SiO ₂) 2008 (Al ₂ O ₃) 2067 (TiO ₂)	(L)		(124) Vorley Rice Mattson Curtis Guin Tarrer
		1870 (SiO ₂) 1875 (Al ₂ O ₃) 1880 (TiO ₂) (sym) (asym) 2096, 2038 (SiO ₂) 2100, 2028 (Al ₂ O ₃) 2100, 2029 (TiO ₂)	(D)	Intense dicarbonyl bands were observed on Al ₂ O ₃ - and TiO ₂ -supported catalysts	
		2043	(L)	in a flowing gas stream with CO/H ₂ ratio equal 3 ν _{CO} = 1996 cm ⁻¹	(127) Dalla Betta Shelef
Ru/Al ₂ O ₃ (5 wt%) 523 K	Precursor: RuCl ₃ R _t : 723 K				
Ru/SiO ₂ 298 K	Precursor: Ru(NO ₃) ₃ R _t : 673 K	2047 (Reduced) 2032 (Oxidized) 2080 (Oxidized) 2144, 2082 (Reduced) (TRI) on Ru ⁺ 2136, 2080 (Oxidized) (TRI) on Ru ⁺	(L) on Ru ⁰ (L) on Rh ⁺ (TRI) on Ru ⁺ (TRI) on Ru ⁺		(128) Yokomizo Louis Bell
Ni/SiO ₂ 298 K	Precursor: Ni(NO ₃) ₂ R _t : 450-550 K	2070-2040 1930 1800	(L) (B) Multicentered species		(129) Primet Daimon Martin

Ni/SiO ₂	Precursor: Ni(NO ₃) ₂	2080, 2040	(L)	(130) Blackmond Ko
300 K	R _t : 773 K	1950	(B)	
Ni/SiO ₂	Precursor: NiCl ₂	2190-2200 2140-2150	weak- (L) on Ni ²⁺ on Ni ⁰	(131) Peri
300 K 10 Torr	R _t : 673-873 K	2110-2120 2020-2085 1960	strong- (L) on Ni ⁰ (ex Cl ⁻) on Ni ⁰ (clean crystals) weak- (B) on Ni ⁰	
Mn/Rh/SiO ₂	Precursor: Rh(NO ₃) ₃ / MnCl ₂ (Mn/Rh= 1.6)	2067 1701 (sym) (asym) 2106, 2020	(L) Mn reduced intensities of the linear and bridged CO bands and caused the bands to shift (B) downward (DI)	(36) Orita Naito Tamaru
300 K 8 Torr				
Na/Rh/SiO ₂	Precursor: RhCl ₃ /Na Aerosil SiO ₂	2056 1830 (sym) (asym) 2092, 2021	(L) Na reduced intensities of the linear and bridged CO bands and caused the bands to shift (B) downward (DI)	(89) Orita Naito Tamaru
300 K 8 Torr				
R/Ru/Al ₂ O ₃	Precursor: Ru ₂ (CO) ₁₀ /	2024 (Ru/Al ₂ O ₃)	(L)	(132) Okukara Tamura Misono
P/Ru/Al ₂ O ₃	K ₂ CO ₃ /P ₂ O ₅	1980 (1 wt%K/Ru/Al ₂ O ₃)		
298 K 60 Torr CO 200 Torr N ₂	O _t : 773 K R _t : 723 K	2040 (1 wt%P/Ru/Al ₂ O ₃)		
Alkaline/Ru/ Al ₂ O ₃	Precursor: Ru ₂ CO ₃ / Li ₂ CO ₃ / Na ₂ CO ₃ / K ₂ CO ₃	2058 (Ru/Al ₂ O ₃) 2050 (Li/Ru=2) - 2050 (Li/Ru=20) 2048 (Na/Ru=2) - 2042 (Na/Ru=20) 2040 (K/Ru=2) - 2028 (K/Ru=20)	The intensity of adsorbed CO bands is reduced on the promoted catalyst	(88) Nori Miyamoto Takahashi Nizuma Hattori Murakami
393 K 15 Torr CO 700 Torr N ₂				

Table 2.4 Infrared Spectroscopy of Hydrocarbon Species

Catalyst/ Preparation	Reaction Condition	Wavenumber (cm ⁻¹)	Assignment/Observation	Reference
Rh/Al ₂ O ₃ Precursor: RhCl ₃ O ₂ : 673 K R _t : 673 K	CO/H ₂	2914	C-H stretching (str.)	(133) Solymosi Tombacz Kocsis
	523 K	1390	C-H deformation (def.)	
	100 Torr	1450, 1210	surface carbonate	
Rh(10 wt%)/Al ₂ O ₃ Precursor: RhCl ₃ O ₂ : 300 K R _t : 473 K	Ethylene Adsorption 300 K	2944	asym. C-H str. of ≡CCH ₃	(134) Beebe Yates
		2886	sym. C-H str. of ≡CCH ₃	
		1407	(CH ₃) asym. def.	
		1344	(CH ₃) sym. def.	
Rh(9 wt%)/Al ₂ O ₃ Precursor: RhCl ₃ O ₂ : 653 K R _t : 653 K	Ethylene Adsorption 200 K 50 Torr	1499	due to π-adsorbed ethylene	(135) Soma
		1410	(CH ₂) asym. def.	
		1214	(CH ₂) sym. def.	
		1444	C=C stretching of π-adsorbed species	
		1460	gasouse C ₂ H ₄	
		1340	C-H deformation vibration of dehydrogenation species	
		1460	C-H deformation vibration of dehydrogenation species	
Rh-Fe(1:0.3)/ SiO ₂ Precursor: RhCl ₃ , FeCl ₃ R _t : 673 K	CO/H ₂ 503 K 51 atm	3014	gas-phase CH ₄	(136) Fukushima Arakawa Ichikawa
		2981 (asym)	CH ₃ str.	
		2804 (sym)		
		2935 (asym)	CH ₃ str.	
		2858 (sym)		
		2958, 2858	methoxyl species [CH ₃ O-Si]	
		1444	methoxy deformation	
		1396	ethoxy deformation	

Ru(5 wt%)/Al ₂ O ₃ CO/H ₂		2928, 2850	saturated C-H (S-CH ₂ -CH ₂ -S)	(127)
Precursor: RuCl ₃	523 K 1 atm	1585(asy) 1378(sym)	0-C-O str. of adsorbed formate ion	Dalla Matte Shelef
R _t : 723 K		1392	C-H def.	
		1460	surface carbonate	
Ru/SiO ₂		2950	methyl group	(23) Ekerdt Bell
Precursor: RuCl ₃	273 K 296 Torr	2910(asy) 2854(sym)	C-H str. in methylene groups	
R _t : 673 K				
Ru/SiO ₂		2960	methyl group	(137) King
Precursor: RuCl ₃	428-523 K	2930 2860	C-H asym. str. in CH ₂ sym. str. in CH ₂	
R _t : 373-723 K				
Ni/SiO ₂		2958	C-H asym. str. in CH ₂	(138) Prinet Sheppard
Precursor: Ni(NO ₃) ₂	adsorption of C ₂ H ₄ on hydrogen-covered Ni/SiO ₂	2925 2878 2860	asym. str. in CH ₂ sym. str. in CH ₂ sym. str. in CH ₂	presence of band above 3000 cm ⁻¹ indicates the presence of =CH- or =CH ₂ group
O _t : 873 K R _t : 623 K				
Al ₂ O ₃		2970	C-H asym. str. in CH ₂	(139) Lucchesi Carter Yates
Precursor: Aluminum Alcohol	ethylene adsorption at 298 K	2930 2880 2853	asym. str. in CH ₂ sym. str. in CH ₂ sym. str. in CH ₂	gaseous ethylene displays IR bands at 3120, 3086, 3006, 2987, 2969 cm ⁻¹ .
R _t : 873 K		1465 1383	C-H asym. bend. in CH ₂ sym. bend. in CH ₂	

terms of symmetric and asymmetric C-H stretching (ν) and C-H deformation (δ). Beebe and Yates [134] studied the reaction of ethylene with Pt, Rh, Pd, and Ru on alumina at 300 K and proposed the surface ethylidyne species, $\text{H}_3\text{C}-\text{CH}$, by infrared spectrum showing the following vibrations: $\nu_a(\text{CH}_3)$ at 2944-2940 cm^{-1} , $\nu_s(\text{CH}_3)$ at 2888-2885 cm^{-1} , $\delta_a(\text{CH}_3)$ at 1411-1397 cm^{-1} , and $\delta_s(\text{CH}_3)$ at 1345-1333 cm^{-1} . The surface methyl group, $\text{H}_3\text{C}-\text{CH}_2$, has been characterized by $\nu_a(\text{CH}_3)$ at 2980-2950 cm^{-1} and $\nu_s(\text{CH}_3)$ at ~ 2905 cm^{-1} . The $\nu_a(\text{CH}_2)$ and $\nu_s(\text{CH}_2)$ of saturated compounds has been characterized by the bands at 2935-2930 cm^{-1} and 2860-2850 cm^{-1} , respectively.


Surface hydrocarbons, such as CH_x intermediates, have been proposed to play an important role in syngas reaction [23-29]. IR has been served to detect the formation of hydrocarbons under reaction conditions, however, the adsorbed hydrocarbon species are commonly overlapped by the gaseous hydrocarbons (Appendix A) which make the presence of surface hydrocarbon species unclear. Several studies attempting to observe F-T intermediates by IR have reported that hydrocarbon species can be removed from the surface by hydrogenation, but did not appear to be an intermediate in hydrocarbon synthesis [23,127,137]. More caution has to be taken to elucidate hydrocarbon intermediates by exclusion of gaseous hydrocarbon species and hydrocarbon spectators.

2.8.2.3 Surface Oxygenates

Acyl species, which is proposed to be an intermediate for oxygenates, has been detected on promoted rhodium catalysts which are active for oxygenate synthesis [36,38,136]. Other surface oxygenates such as formate and carboxylate species have also been reported

[14,127,140]. Table 2.5 lists the vibrational frequency of these oxygenates on different catalyst surfaces. Identification of the intermediate oxygenate may help to elucidate the reaction pathway.

Table 2.5 Infrared Spectroscopy of Oxygenate Species

Catalyst	Reaction Condition	Wavenumber (cm ⁻¹)	Assignment	Ref.
Mn(1)/Rh/SiO ₂ Precursor: RhCl ₃ /MnCl ₂ R _t : 673 K	CO/H ₂	1735	Physisorbed acetaldehyde	(136) Fukushima Arakawa Ichikawa
	230-250 K 29 atm	1683-1672	CH ₃ C=O	
		1564, 1442	Bidentate acetate (O-C-O)	
			CH ₃ 	
Mn/Li/Rh/SiO ₂ (Mn:Li:Rh = 0.08:0.6:1.0) R _t : 723 K	CO/H ₂	1745 1444	Monodentate acetate	(14) Arakawa Fukushima Ichikawa
	553 K 50 atm	1382	(ester group)	
		1579 1444	Bidentate acetate	
			CH ₃ C=O O	
La(5)/Rh/SiO ₂ Precursor: RhCl ₃ /La(NO ₃) ₃ R _t : 573 K	CO/H ₂	1680	Acyl	(38) Underwood Bell
	530 K 12 atm	1580 1370	Formate O-C-O (asym) (sym)	
		1555 1440	O-C-O (asym) (sym)	
Rh/Al ₂ O ₃ Precursor: RhCl ₃ O _t : 673 K R _t : 673 K	CO/H ₂	1595	O-C-O (asym)	(133) Solymosi Tomacz Kocsis
	523 K	1380	(sym)	

<p>Mn(1.5)/Rh/SiO₂ Precursor: Rh(NO₃)₃/MnCl R_t: 473-723 K</p>	CO/H ₂	1745	Acyl	(36)
	523 K	1720	Ester group	Orita
	250 Torr	1568	0-C-O (asym)	Naito
		1414	(sym)	Tamaru
<p>Ru/Al₂O₃ Precursor: RuCl₃ R_t: 723 K</p>	formic acid adsorption at 523 K	1585	0-C-O (asym)	(127)
		1378	(sym)	Dalla Betta
		1392	C-N def. of surface formate	Shelef
<p>Ni/SiO₂ Precursor: Ni(NO₃)₂ R_t: 703 K</p>	formic acid adsorption	1587	0-C-O (asym)	(140)
		1350	(sym)	Dlyholder
	acetic acid adsorption	1578	0-C-O (asym)	Shihabi
		1443	CH ₃ def.	Wyatt
		1430	0-C-O (sym)	Nartlett
		1414	CH ₃ def.	

CHAPTER III

EXPERIMENTAL

3.1 Catalyst Preparation and Characterization

The catalysts were prepared by impregnation and co-impregnation. Rhodium(III) chloride ($\text{RhCl}_3 \cdot 3\text{H}_2\text{O}$) and ruthenium(III) chloride ($\text{RuCl}_3 \cdot 1\sim 3\text{H}_2\text{O}$) were obtained from Alfa Products. Nickel(III) nitrate ($\text{Ni}(\text{NO}_3)_3 \cdot 6\text{H}_2\text{O}$) and silver(I) nitrate (AgNO_3) were supplied by Johnson Matthey Chemicals. Silica supports used were provided by Strem Chemicals Company (#14-7420, pore volume: $1.7 \text{ cm}^3/\text{g}$, surface area: $350 \text{ m}^2/\text{g}$). The desired amount of the salts were dissolved in distilled water that was used to fill up the pores of the silica. After impregnation, the sample was dried overnight in air at room temperature. The dried sample was then heated in flowing hydrogen to 673 K with heating rate of 2 K/min and reduced at 673 K for 16 hr.

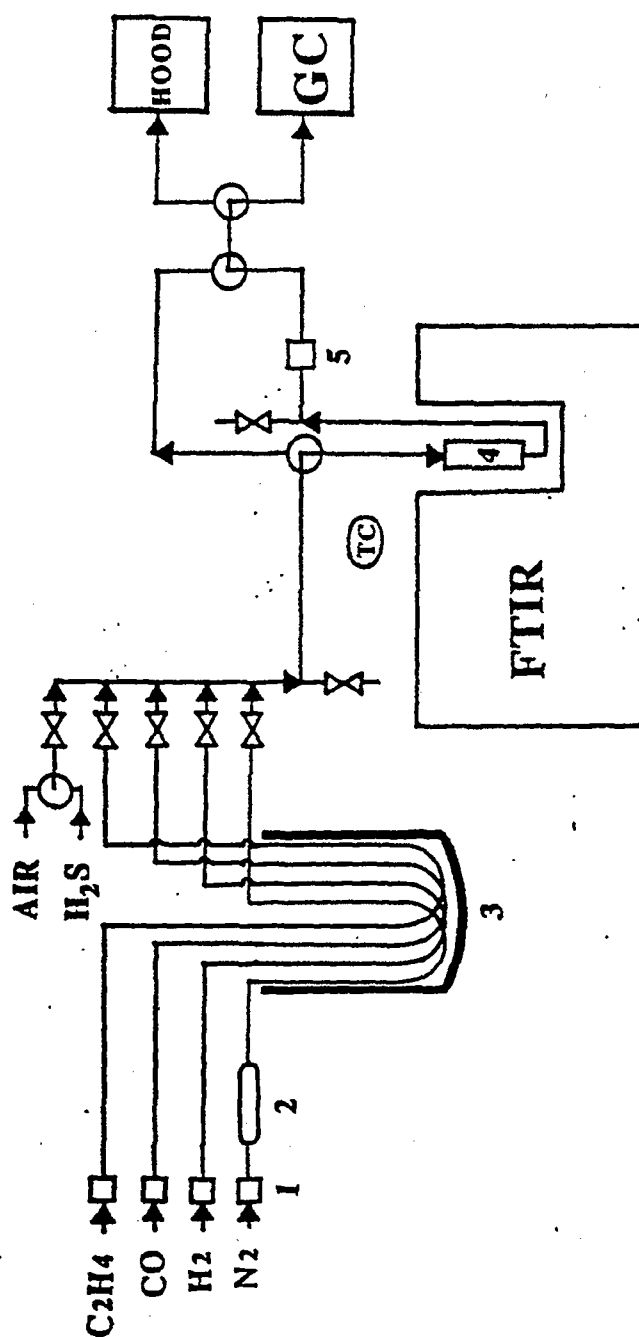
Metal loading of supported metal was verified by X-ray fluorescence (XRF); metal crystallite size of the catalysts was determined by X-ray diffraction (XRD); and the oxidation state of supported metals was determined by X-ray photoelectron spectroscopy (XPS) before or after the reaction. Adsorption of CO on catalysts was used to characterize the state of catalyst surfaces during the reaction.

3.2 Reactor System

Figure 3.1 shows the apparatus of the reactor system. Nitrogen (UHP grade), hydrogen (UHP grade), carbon monoxide (CP grade), and ethylene (CP grade) were supplied by Linde Corporation. The gaseous feed were passed through liquid N_2 trap to remove residual water. Nitrogen was further passed through a de-oxo and a dehydrating unit (Supelco). Gas flows were regulated with Brooks Mass Flow Controller. Hydrogen sulfided and air were introduced when sulfidation and oxidation were necessary. Hydrogen sulfur, supplied by Matheson Gas Products, was 1000 ppm H_2S with a mixture of hydrogen. Air was passed through a de- CO_2 and dehydrating unit (Balston) before used.

The reduced catalyst samples were pressed into a self-supporting disk (10 mm in diameter, and 1 mm in thickness) with a pressure of 470 MPa and then placed in an IR cell. The IR cell, as shown in Figure 3.2, consists of four stainless-steel flanges, a gas inlet and outlet, and two step CaF_2 windows. The step windows minimize the reactor volume and reduce the optical path length for the gaseous species in the reactor. The reactor temperature was controlled by Omega Temperature Controller (Model 2011k) from room temperature to 513 K. A back pressure regulator (Veriflo) at the outlet of the IR cell maintained the reactor pressure up to 30 atm.

CO hydrogenation ($CO:H_2=1:1$) and ethylene hydroformylation ($CO:H_2:C_2H_4=1:1:1$) were performed over the catalyst disk in the IR cell under 373-513 K and 1-30 atm. Space velocities of 7500 to 11000 hr^{-1} were used to keep CO conversion below 5%. Due to the use of a small amount of catalyst in the IR cell, the IR cell reactor can be



1. mass flow controller 2. de-oxo and dehydrating unit 3. liquid N_2 trap
4. IR cell 5. back pressure regulator

Figure 3.1 Schematic Diagram of the Experimental Apparatus.

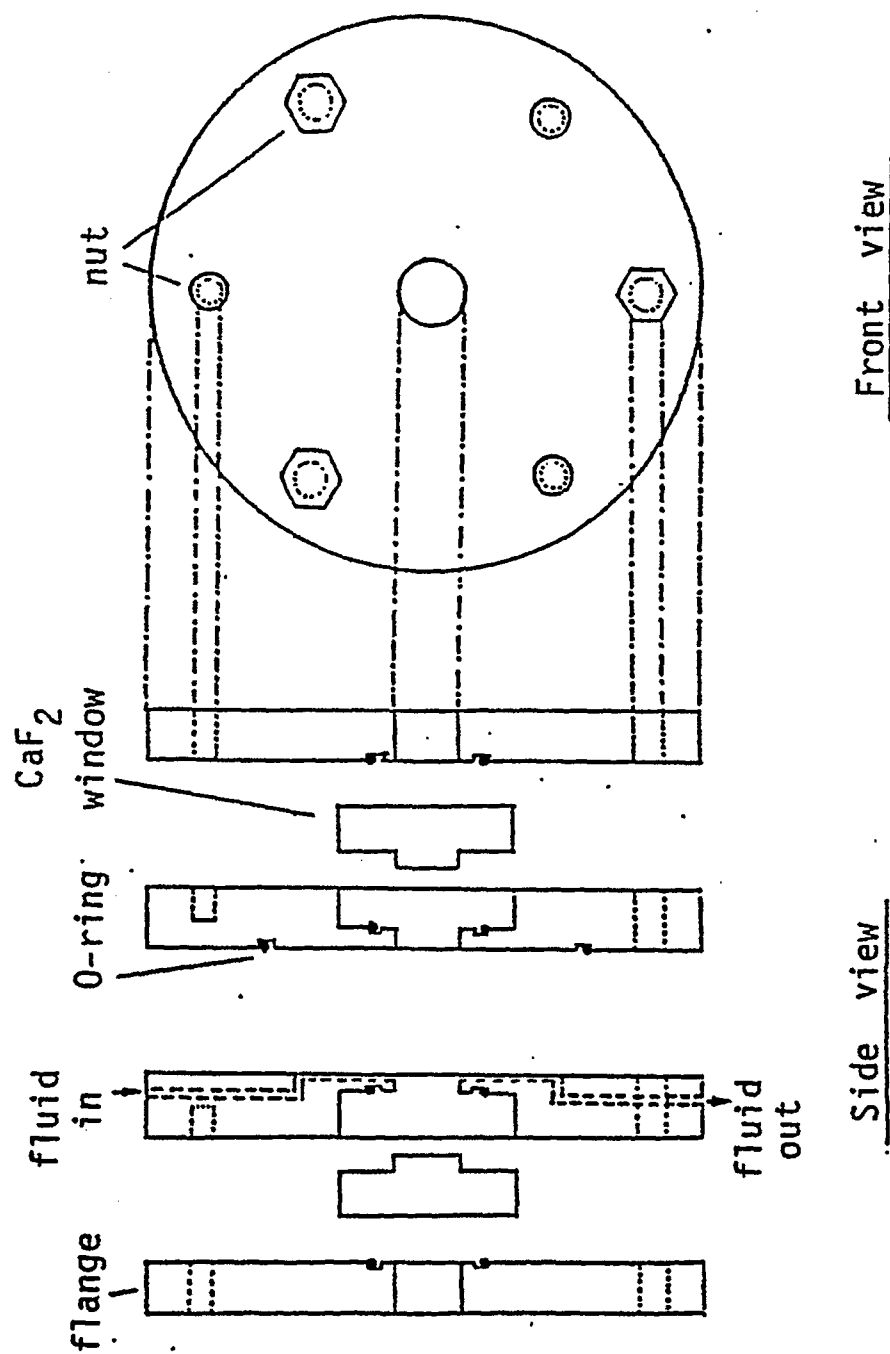


Figure 3.2 High Pressure IR Cell for in situ IR Studies.

considered to be a differential reactor. Heat and mass transfer effects of the reactor is minimized. 39

Infrared spectra were measured by a Nicolet 5XSC FTIR spectrometer with a DTGS detector at a resolution of 4 cm^{-1} . The effluent of the IR cell was sampled during the reaction and was analyzed by an on-line gas chromatography (HP-5890A) with a 6 ft Porapak PS column in series with a 6 ft Porapak QS column.

CHAPTER IV
INFRARED STUDY OF THE CO INSERTION REACTION ON REDUCED,
OXIDIZED, AND SULFIDED Rh/SiO₂ CATALYSTS

4.1 Introduction

The insertion of carbon monoxide (CO) into a metal-carbon σ bond is one of the most widely studied reactions in organometallic chemistry [45,46]. The interest in CO insertion stems from the fact that the reaction provides a pathway for the conversion of olefins or other substrates to high added-value chemicals [46,51]. Homogeneous hydroformylation processes have been the largest industrial application of the CO insertion chemistry for more than three decades [46-49]. Although Rh carbonyls and complexes are the most active hydroformylation catalysts, mechanistic information about CO insertion has commonly been obtained using metals such as Mn, Ir, or Pt which form unreactive and stable acyl complexes [141]. The use of these organometallic complexes allows for close observation of how the migratory CO insertion occurs. Infrared study of the ¹³CO insertion on alkyl(pentacarbonyl)-manganese has provided direct evidence for the migratory insertion of CO into a carbon-metal bond on Mn⁺ [50]. The rate of CO insertion on methyl-(pentacarbonyl)manganese can be further accelerated by a Lewis acid [142].

It has been suggested that the migratory CO insertion plays ⁴¹ a key role in the Fischer-Tropsch (F-T) synthesis [47-49]. Pichler et al. first used CO insertion as a model for rationalization of chain growth in the F-T catalysis on surfaces [143]. However, most F-T studies over the past decade have shown that CO insertion is not the major pathway for the chain propagation of adsorbed alkyl [8,20,22]. The CO insertion step was found to be the chain termination step leading to the formation of aldehydes and alcohols [56,39,57].

While it has been well established that CO insertion occurs via the migration of an alkyl group to a Rh^+ -coordinated CO in homogeneous catalysis [45-50], much controversy exists concerning active sites for CO insertion in the CO hydrogenation reaction (F-T synthesis). Watson and Somorjai proposed that CO insertion to form C_2 oxygenates occurs on the Rh^+ sites while CO dissociation takes place on the reduced Rh^0 sites [58,59]. The postulate has been further supported by a number of studies [39,64,65]. On the contrary, Katzer et al. [67] reported from an XPS study that there was no evidence for the existence of Rh^+ on Rh/TiO_2 which was active for the synthesis of C_2 oxygenates. A number of studies have shown no correlation of C_2 oxygenate activity to the amount of Rh^+ or Rh^{2+} ions present on the Rh catalysts [66,68].

The present study was aimed at identification of the type of adsorbed CO species which participates in the CO insertion step in ethylene hydroformylation. The Rh catalyst system chosen for this study comprises three different forms of Rh: reduced Rh, oxidized Rh, and sulfided Rh. The types of CO adsorbed on these Rh surfaces are closely related to the surface states of Rh [119-125]. Infrared data for CO adsorption on these Rh catalysts under various reaction

conditions were obtained to determine the type of adsorbed CO for CO insertion and to shed light on the nature of active sites for the reaction.

42

4.2 Experimental

4.2.1 Catalyst Preparation and Characterization

A 3 wt% Rh sample was prepared by impregnation of SiO_2 with an aqueous solution of $\text{Rh}(\text{NO}_3)_3 \cdot 2\text{H}_2\text{O}$. The procedure of the preparation is described in Chapter III. The crystallite size of Rh was determined to be 96 Å by hydrogen chemisorption. The reduced Rh/ SiO_2 sample was pressed into a self-supporting disk with 20 mg.

The catalyst disk in the IR cell was subjected to further treatments prior to the adsorption and reaction studies. The treatments included reduction, oxidation, and sulfidation. The catalyst disk reduced in H_2 flow at 513 K for 1 hr is designated as the reduced Rh/ SiO_2 catalyst; the catalyst disk oxidized in flowing air at 513 K for 1 hr is denoted as the oxidized Rh/ SiO_2 catalyst; and the catalyst disk sulfided in H_2S flow (1000 ppm H_2S in H_2) at 513 K for 1 hr is designated as the sulfided Rh/ SiO_2 catalyst. Sulfur content of the sulfided Rh was measured by X-ray fluorescence spectroscopy. The oxidation state of the Rh surface on the reduced and oxidized catalysts was determined by X-ray photoelectron spectroscopy (XPS) using a Leybold LHS-10 surface analysis system.

4.2.2 Experimental Procedure

CO adsorption was conducted by exposing the catalysts to 1-10 atm of CO at 301 K. Gaseous CO was removed by flowing nitrogen. The infrared spectra of adsorbed CO were recorded at 1 atm. The reactivity of the adsorbed CO was investigated by introducing $\text{C}_2\text{H}_4/\text{H}_2$ (molar ratio

of $C_2H_4:H_2 = 1:1$) to the adsorbed CO in the IR cell which served as ⁴³ batch reactor. The reaction of the preadsorbed CO with C_2H_4 and H_2 was carried out at 301 K and a pressure of slightly above 1 atm. The infrared spectra of adsorbed CO and intermediates during the reaction was measured as a function of reaction time.

Steady-state ethylene hydroformylation over the reduced, oxidized, and sulfided Rh/SiO₂ catalysts was carried out in the IR cell at 373-513 K and 1-10 atm. Infrared spectra were recorded as a function of time on stream. The effluent of the IR cell was sampled after 40 min at each reaction condition and was analyzed by the on-line gas chromatograph.

4.3 Results

4.3.1 X-Ray Photoelectron Spectroscopy

Figure 4.1 shows the XPS spectra of the Rh/SiO₂ following different treatments. The Rh 3d_{3/2} and 3d_{5/2} binding energies for the Rh/SiO₂ after exposure to air were observed at 312.3 and 307.5 eV, respectively. Following the reduction at 513 K, the Rh surface was reduced as indicated by the downshift of 0.8 - 0.9 eV. Subsequent oxidation in air at 513 K shifted the Rh 3d_{3/2} and 3d_{5/2} binding energies back to 312.2 and 307.6 eV. The difference of 0.8-0.9 eV in binding energy between the reduced and oxidized Rh/SiO₂ clearly indicates that the Rh surface on the reduced Rh/SiO₂ contains primarily Rh⁰ atoms; and the Rh surface on the oxidized Rh/SiO₂ comprises mainly Rh⁺ ions.

4.3.2 CO Adsorption

Figure 4.2 shows the infrared spectra of CO adsorption on the reduced Rh/SiO₂ at 301 K. Two intense bands at 2073 and 1898 cm⁻¹ are

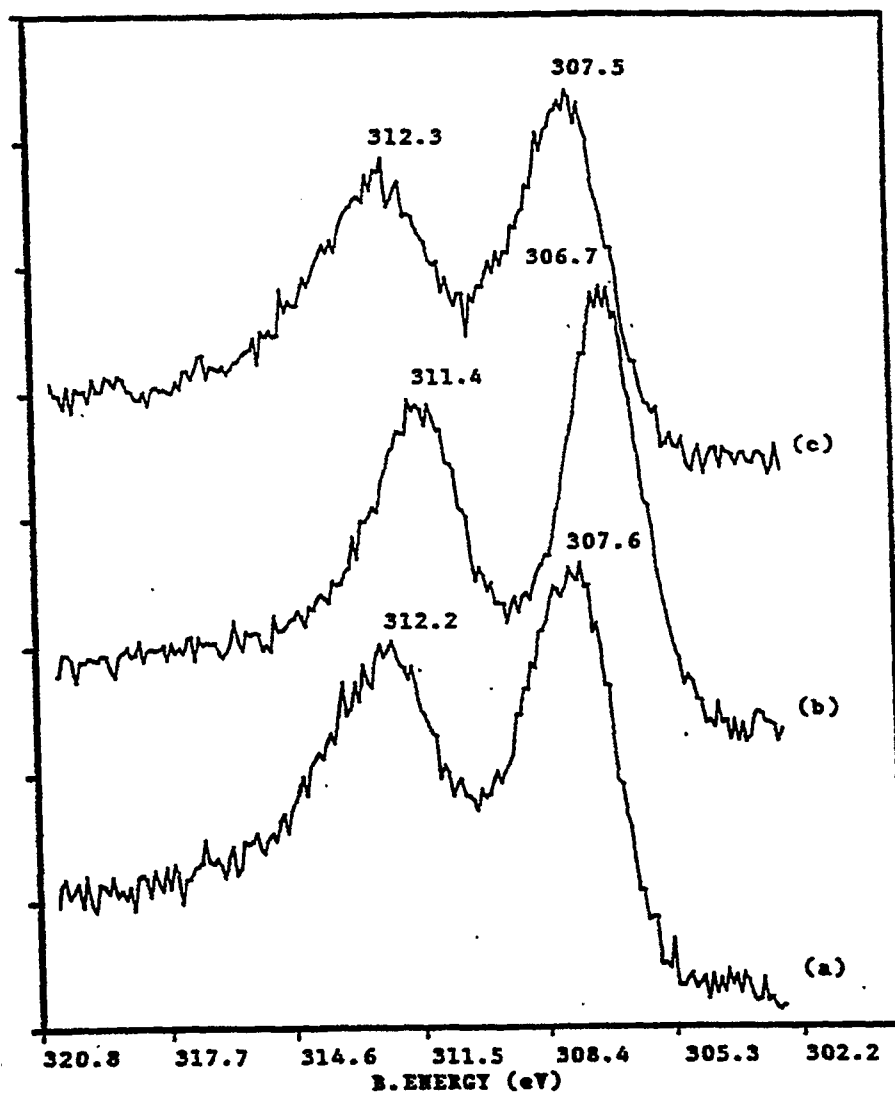


Figure 4.1 Rh $3d_{3/2}$, $3d_{5/2}$ XPS Spectra of Rh/SiO₂: (a) after exposure to air at room temperature, (b) after reduction in H₂ at 513 K for 3 hr, (c) after oxidation in air at 513 K for 3-hr.

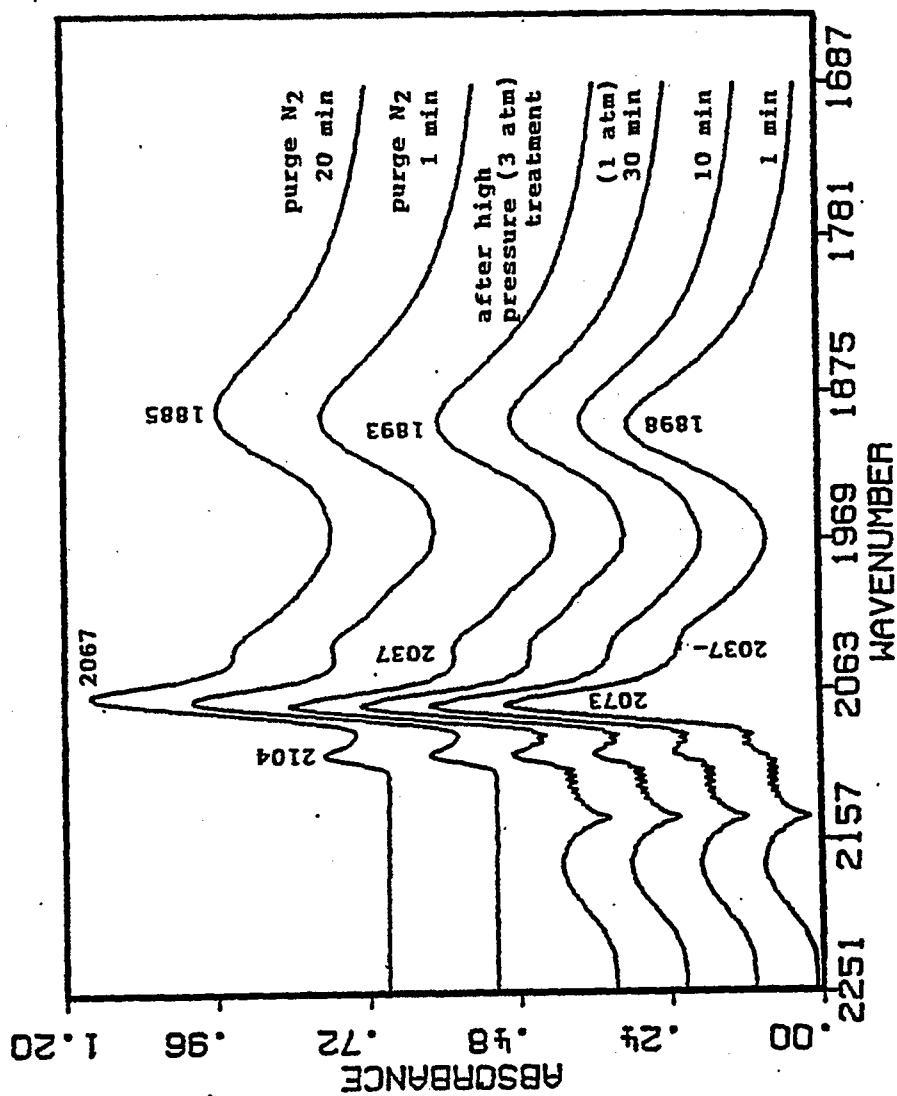


Figure 4.2 CO Adsorption on the Reduced Rh/SiO₂ Catalyst at 301 K.

assigned to the linear (terminal) and bridged CO adsorbed on the reduced Rh crystallite surface, respectively. The small band at 2104 cm^{-1} and the shoulder at 2037 cm^{-1} are attributed to the symmetrical and asymmetrical C-O stretching of $\text{Rh}^+(\text{CO})_2$, the rhodium gem-dicarbonyl. Assignments of these adsorbed CO species agree well with those reported for CO adsorption on supported Rh [119-125].

The intensity of the gem-dicarbonyl bands slowly increased with exposure time, but the intensity of the bridged CO band remained essentially constant. A further increase in the intensity of the gem-dicarbonyl bands was observed after exposing the catalyst to 3 atm of CO. The slow development of gem-dicarbonyl has been attributed to the disruption of Rh crystallites and the formation of isolated Rh^+ sites [122]. Removal of gaseous CO by flowing nitrogen caused decreases in the intensity and wavenumber of linear CO and bridged CO bands. The decrease in the CO wavenumber has been attributed to the decrease in dipole-dipole interactions between adsorbed CO species [118].

Figure 4.3 shows the infrared spectra of CO adsorption on the oxidized Rh/SiO_2 at 301 K. The band at 2096 cm^{-1} developed and shifted to 2101 cm^{-1} as exposure time increased. A low intensity band at 2025 cm^{-1} also increased in intensity with exposure time. Exposing the catalyst to 10 atm of CO produced a complex infrared spectrum. The development of various IR bands for adsorbed CO species can be clearly discerned in the difference spectra, shown in Figure 4.4, which highlights the difference between successive spectra in Figure 4.3. The upward shift of the 2096 cm^{-1} band as the intensity increased indicates that the band is not completely due to the symmetric

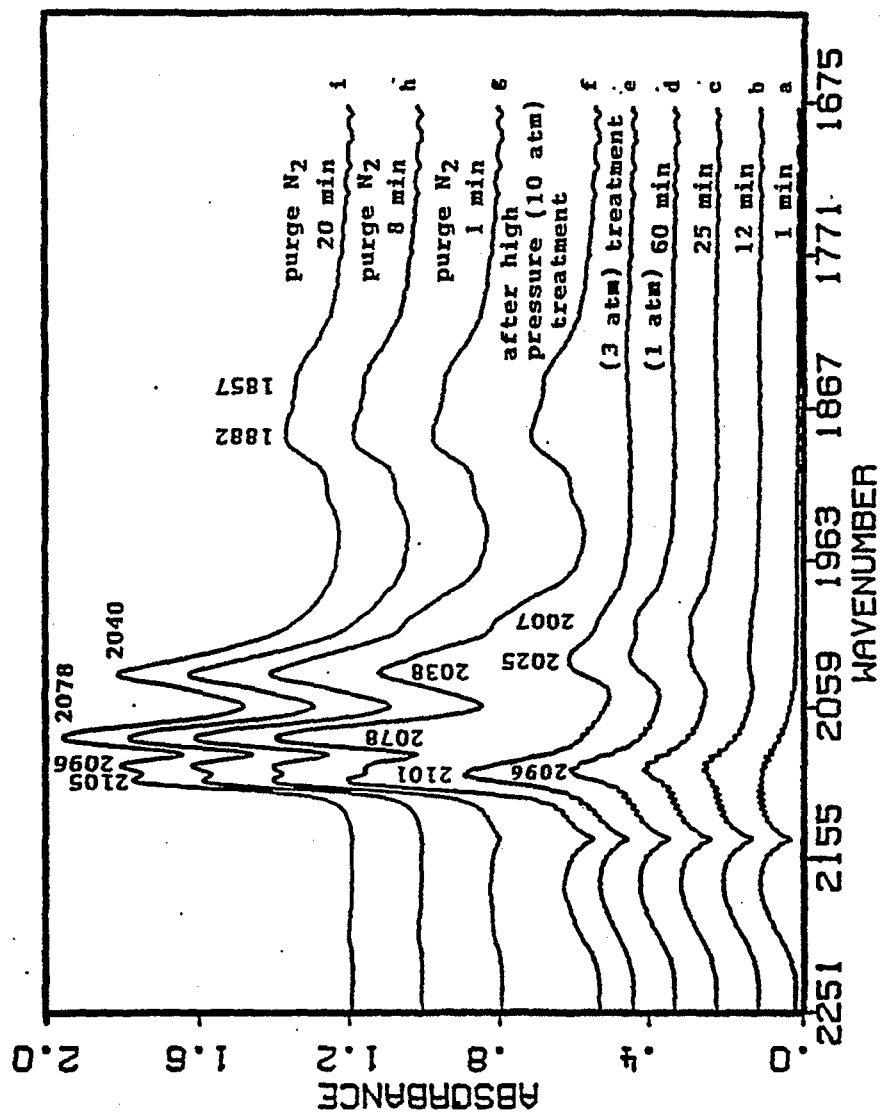


Figure 4.3 CO Adsorption on the Oxidized Rh/SiO₂ Catalyst at 301 K.

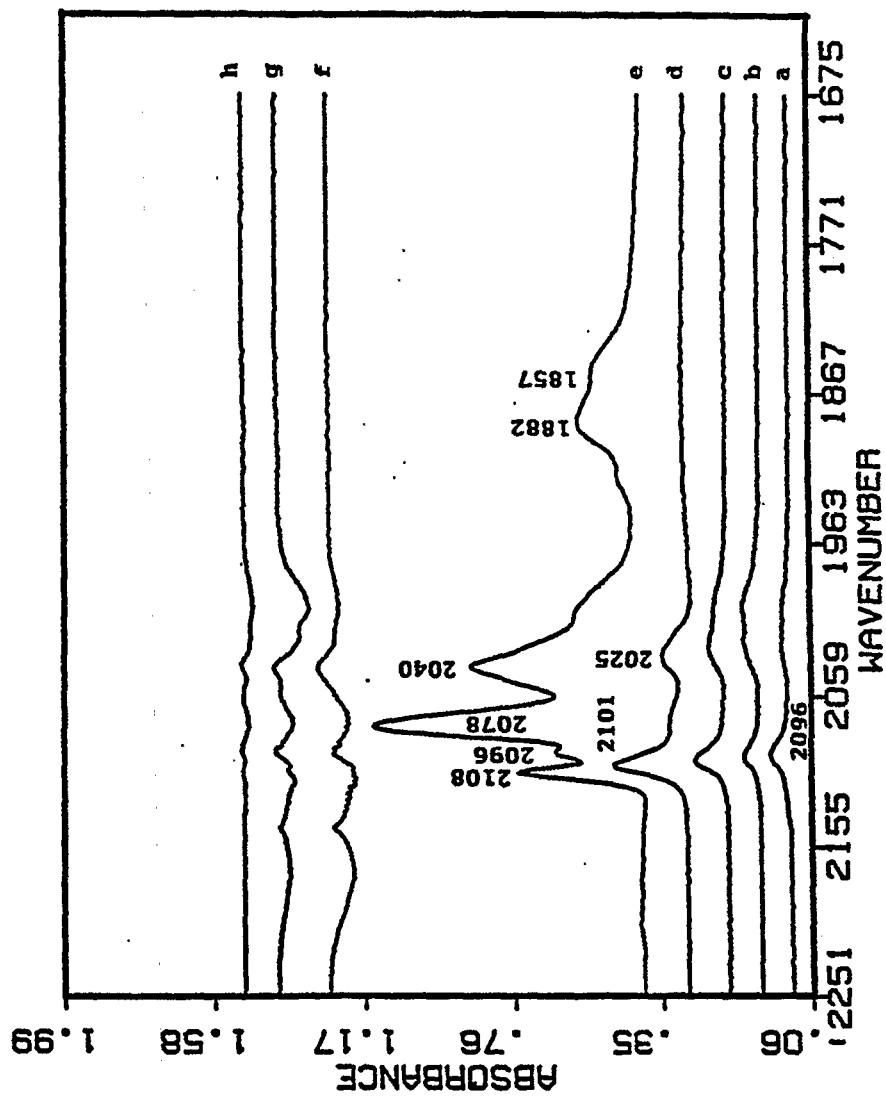


Figure 4.4 Sequential Difference Spectrum of CO Adsorption: obtained from subtraction of spectra in figure 3; spectrum 4a= 3b-3a, spectrum 4b= 3c-3b, spectrum 4c= 3d-3c, etc.

vibration of $\text{Rh}^+(\text{CO})_2$ because the wavenumbers of symmetric and asymmetric bands of $\text{Rh}^+(\text{CO})_2$ do not change with their intensities [119-121]. The 2096 cm^{-1} band is assigned to the linear CO adsorbed on the Rh^+ ions. Linear CO adsorbed on Rh^+ is known to give an IR band in the $2100\text{--}2090\text{ cm}^{-1}$ region [119-125]. Part of the 2096 cm^{-1} band may be due to the symmetric vibration of $\text{Rh}^+(\text{CO})_2$ which also gave rise to the asymmetric vibration at 2025 cm^{-1} . The complex spectrum resulting from exposure to 10 atm of CO consists of bands at 2108, 2096, 2078, 2040, 2007, 1882, and 1857 cm^{-1} . The species is quite stable in nitrogen flow. The spectrum does not match with the spectra of various types of Rh carbonyls such as $\text{Rh}_4(\text{CO})_{12}$ and $\text{Rh}_6(\text{CO})_{16}$ [48]. The structure of the resulting complex remains unclear.

Figure 4.5 shows the infrared spectra of CO adsorption on the sulfided Rh/SiO_2 catalyst at 301 K. CO adsorption produced a band at 2090 cm^{-1} which may be assigned to a linearly adsorbed CO. Exposure of the sulfided catalyst to CO for 60 min resulted in an increase in the intensity of the linear CO band and an upward shift of its wavenumber to 2095 cm^{-1} . Two bands at 2029 and 2005 cm^{-1} are due to the weakly adsorbed CO on the catalyst surface as indicated by the decreasing intensity of these bands in flowing nitrogen.

4.3.3 Reaction of Adsorbed CO with C_2H_4 and H_2

Figure 4.6 shows the infrared spectra taken during the reaction of C_2H_4 and H_2 with the preadsorbed CO on the reduced Rh/SiO_2 catalyst at 301 K. The infrared spectrum prior to admission of $\text{C}_2\text{H}_4/\text{H}_2$ exhibited linear CO band at 2070 cm^{-1} , bridged CO band at 1891 cm^{-1} , and gem-dicarbonyl bands at 2104 and 2040 cm^{-1} . Exposure of adsorbed CO to $\text{C}_2\text{H}_4/\text{H}_2$ decreased the intensity and wavenumber of the linear CO

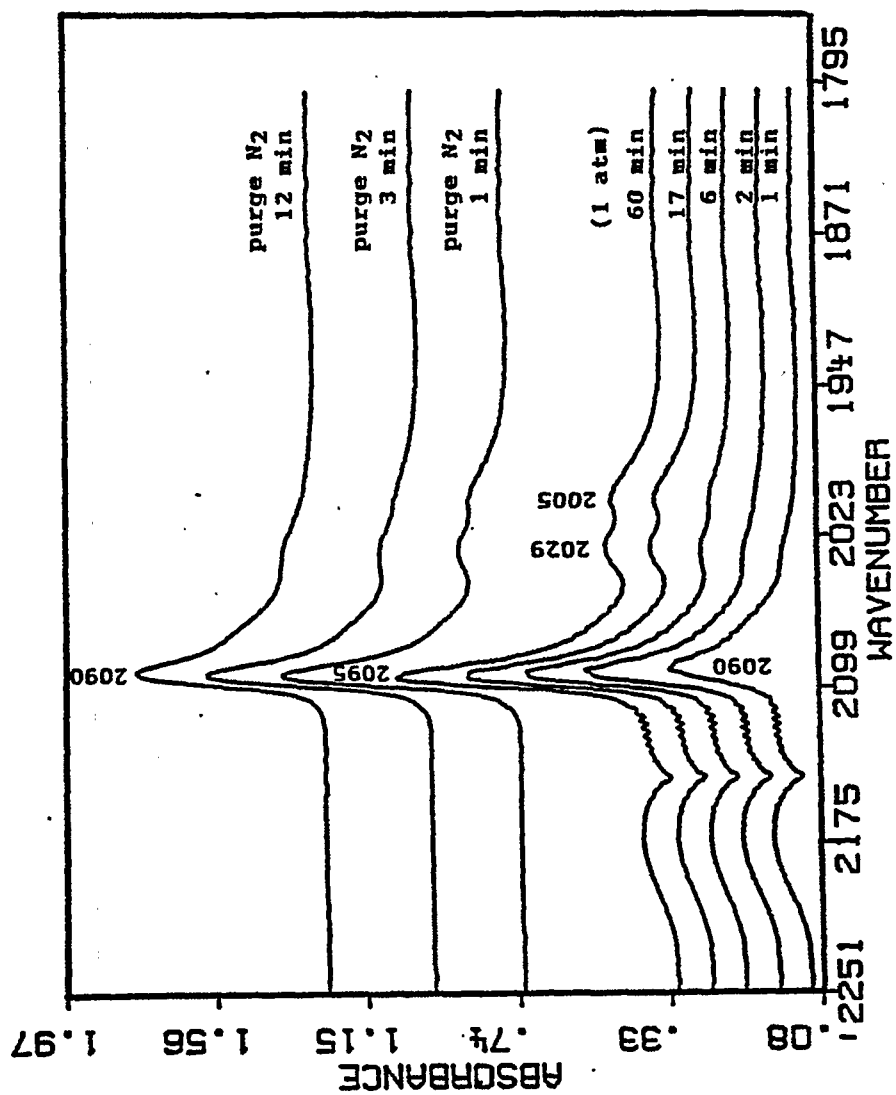


Figure 4.5 CO Adsorption on the Sulfided Rh/SiO₂ Catalyst at 301 K.

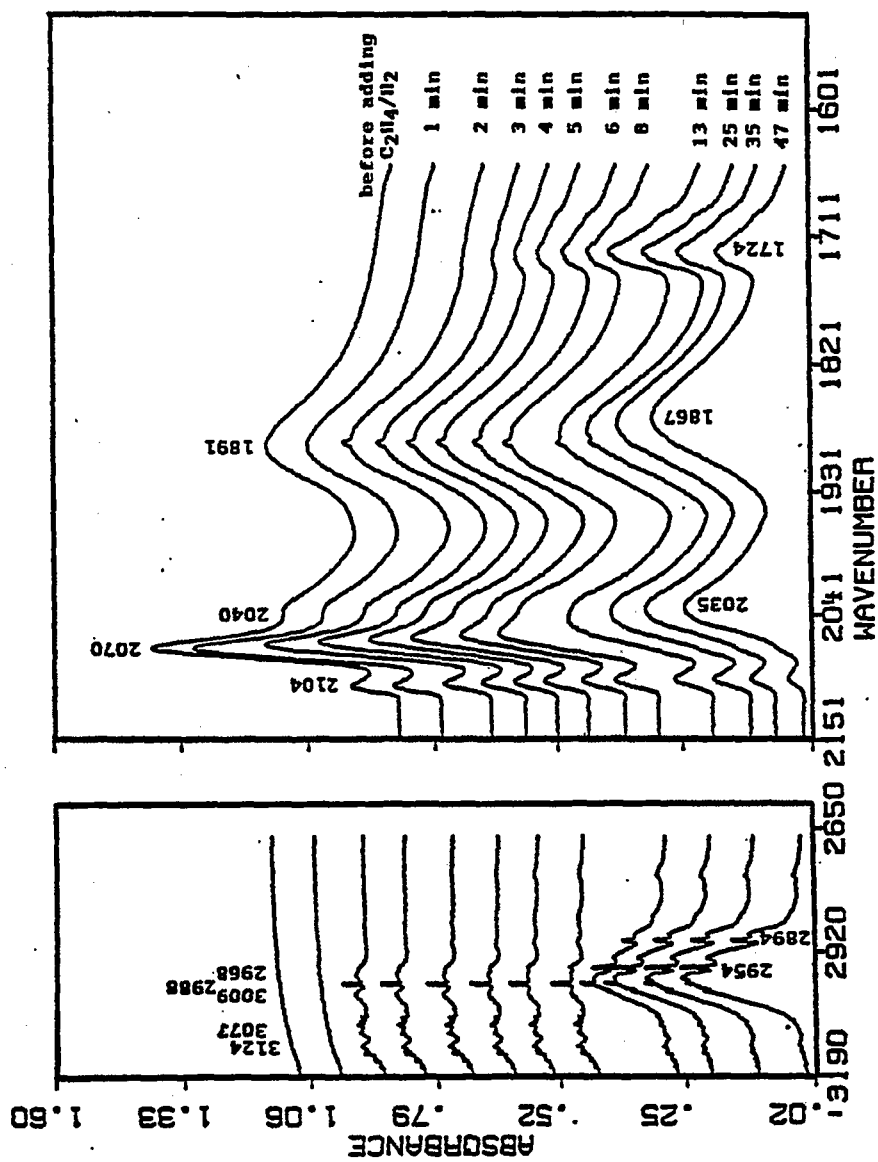


Figure 4.6 Reaction of $\text{C}_2\text{H}_4/\text{H}_2$ with Adsorbed CO on the Reduced Rh/SiO₂ Catalyst at 301 K.

band at 2070 cm^{-1} . At the same time, the propionaldehyde band at 1724 cm^{-1} emerged. A slight decrease in the intensity of gem-dicarbonyl bands was also observed. The consumption of linear CO and the formation of propionaldehyde indicate that the linear CO adsorbed on the Rh^0 crystallite is the major type of adsorbed CO which participates in CO insertion leading to the formation of propionaldehyde at 301 K and 1 atm. The spectra for hydrocarbons in the $2650 - 3200\text{ cm}^{-1}$ region show that ethylene bands at 3124, 3077, and 2988 cm^{-1} depleted as ethane bands near 2954 and 2894 cm^{-1} increased in intensity. The simultaneous formation of propionaldehyde and ethane indicates that the insertion of CO into adsorbed ethylene competes with ethylene hydrogenation.

Figure 4.7 shows the reaction of C_2H_4 and H_2 with the preadsorbed CO on the oxidized Rh/SiO_2 catalyst at 301 K. The infrared spectrum of adsorbed CO prior to exposure to C_2H_4 and H_2 is identical to that shown in Figure 4.3. Admission of $\text{C}_2\text{H}_4/\text{H}_2$ to the preadsorbed CO resulted in the formation of the propionaldehyde band at 1732 cm^{-1} and a band at 1632 cm^{-1} , and a dramatic variation of CO bands in the $2105\text{-}1860\text{ cm}^{-1}$ region. No bands which can be attributed to an adsorbed acyl species or complex were observed. The 1631 cm^{-1} band may be assigned to the carboxylate species of which carbon attaches on two oxygen atoms [117]. The role of this species in the propionaldehyde formation remained unclear.

The change in IR spectra of adsorbed CO upon admission of $\text{C}_2\text{H}_4/\text{H}_2$ and during the reaction can be clearly discerned by the difference spectra as shown in Figure 4.8. The difference spectrum 4.8-a shows a very complex pattern which is the mirror image of

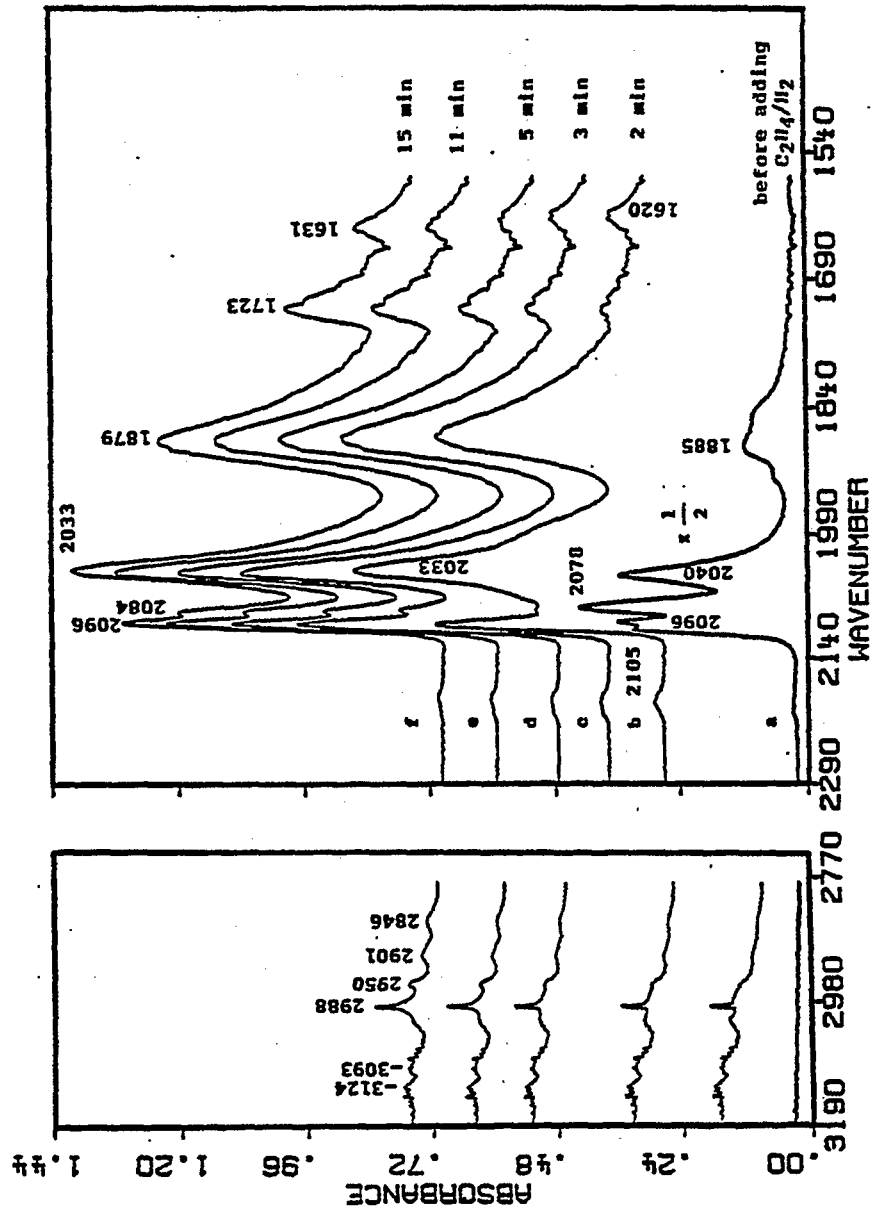


Figure 4.7 Reaction of $\text{C}_2\text{H}_4/\text{H}_2$ with Adsorbed CO on the Oxidized Rh/SiO₂ Catalyst at 301 K.

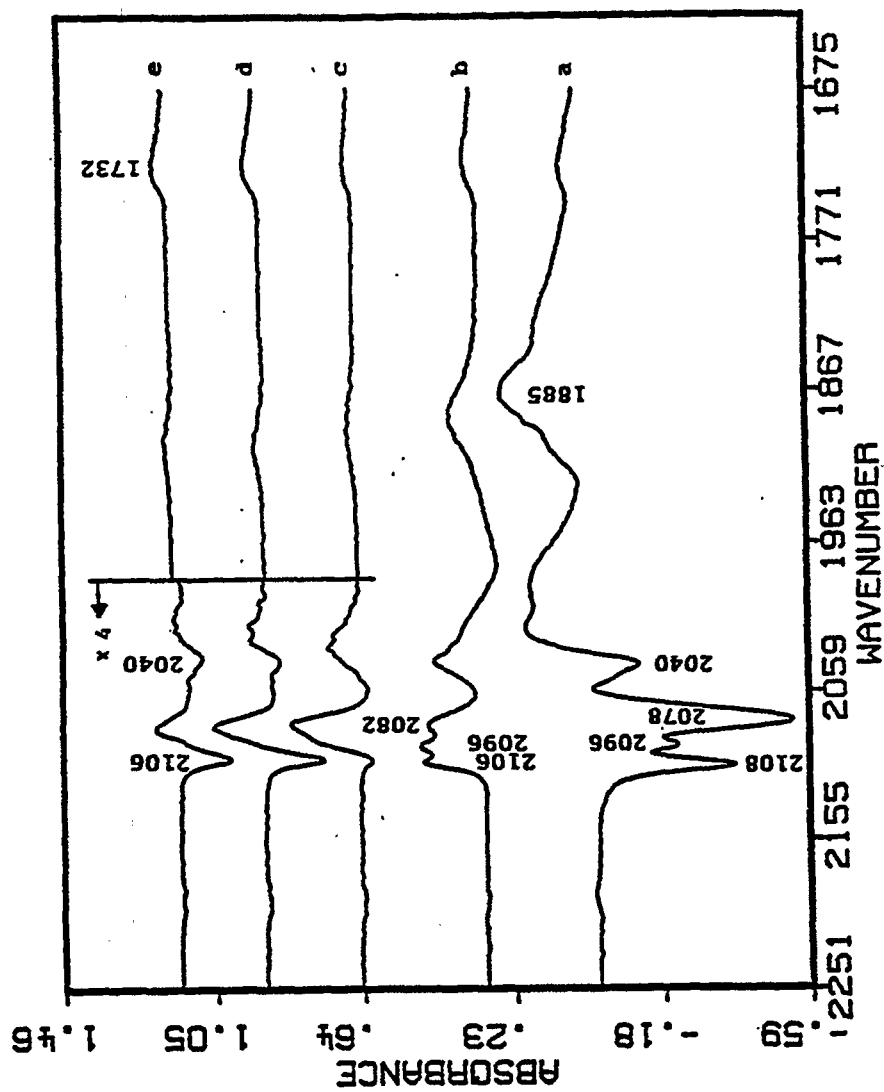


Figure 4.8 Sequential Difference Spectrum of the Reaction of C_2H_4/H_2 with Adsorbed CO: obtained from subtraction of spectra in figure 7; spectrum 8a= 7b-7a, spectrum 8b= 7c-7b, spectrum 8c= 7d-7c, etc.

spectrum 4.4-e. The unknown species exhibiting the complex spectrum disappeared upon admission of C_2H_4 and H_2 . The species appears to be unstable under reaction conditions; its relation to propionaldehyde formation remains unclear. A clear relationship between the variation of adsorbed CO and the formation of propionaldehyde can be observed after 3 min of the reaction. The decrease in the intensity of the band at 2105 cm^{-1} appears to correlate to the increase in the intensity of the propionaldehyde band at 1732 cm^{-1} , suggesting that the linear CO adsorbed on the Rh^+ site is involved in CO insertion leading to the formation of propionaldehyde.

Figure 4.9 shows the changes of infrared spectra taken during the interaction of C_2H_4 and H_2 with preadsorbed CO on the sulfided Rh/SiO_2 catalyst at 301 K. The intensity of the linear CO at 2091 cm^{-1} decreased upon the addition of C_2H_4 and H_2 . Neither detectable propionaldehyde nor ethane was observed during the entire period of the reaction study. The lack of activity of the sulfided catalyst for catalyzing propionaldehyde and hydrocarbon formation may be due to a strong inhibition of ethylene and hydrogen adsorption brought about by adsorbed sulfur at 301 K.

4.3.4 Steady State Ethylene Hydroformylation

Figure 4.10 shows the infrared spectra for ethylene hydroformylation on the reduced Rh/SiO_2 catalyst. The rate of product formation corresponding to the infrared spectra are presented in Table 4.1. Ethane was the major product; methane and propionaldehyde were minor products at 373 K and 1 atm. Under the same reaction condition, the infrared spectrum shows the prominent linear CO band at 2042 cm^{-1} and the bridge CO band at 1871 cm^{-1} . Increasing temperature from 373

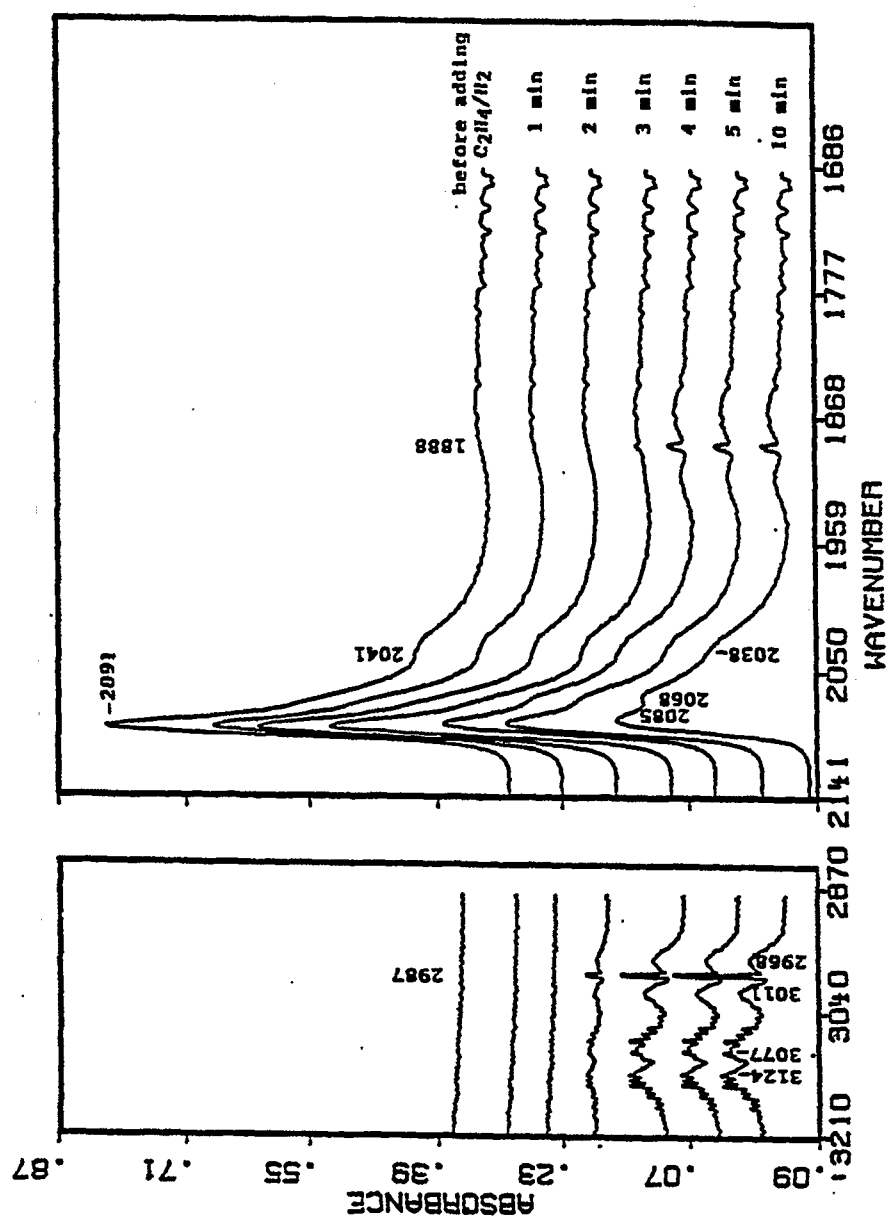


Figure 4.9 Reaction of C_2H_4/H_2 with Adsorbed CO on the Sulfided Rh/SiO_2 Catalyst at 301 K.

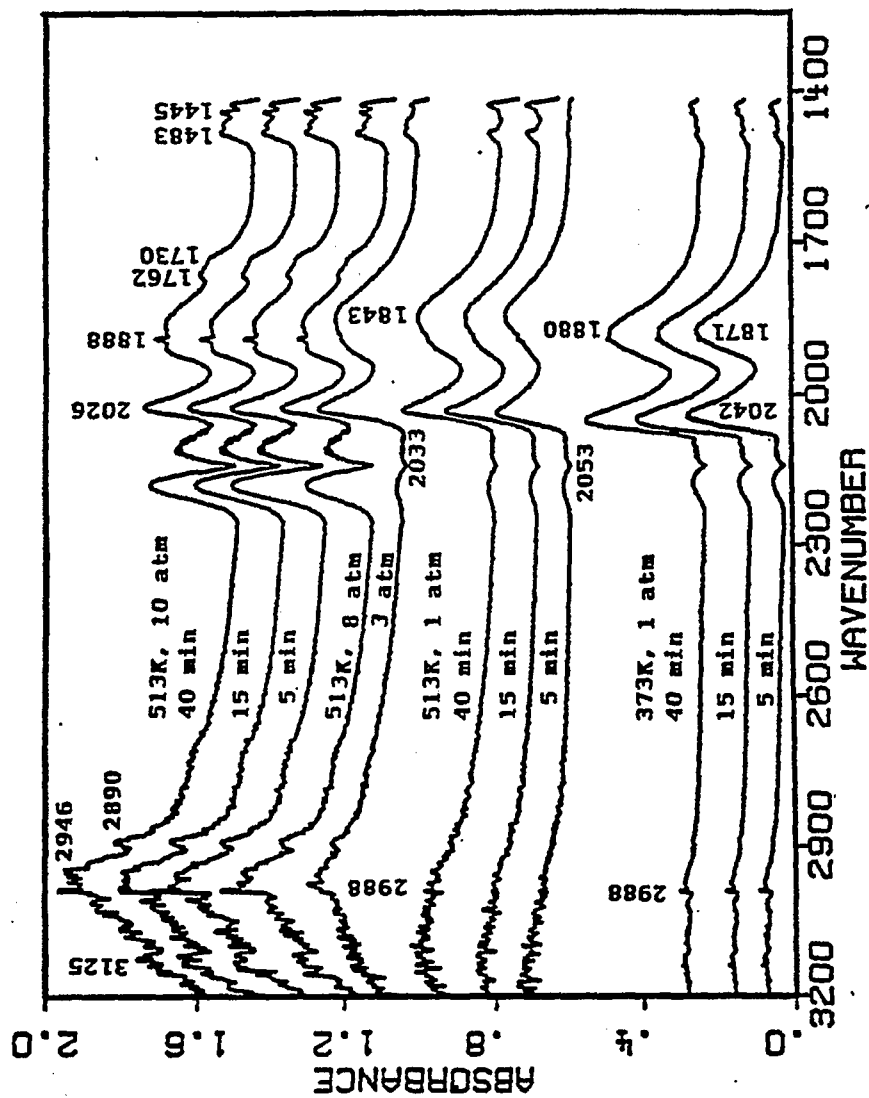


Figure 4.10 Ethylene Hydroformylation on the Reduced Rh/SiO₂.

Table 4.1 Rates of Products of Ethylene Hydroformylation over Reduced, Oxidized, and Sulfided Rh/SiO₂ Catalysts

Catalyst/Reaction Condition	Rate of product formation (mole/Kg-hr)					$\frac{C_2H_5CHO^a}{C_2H_6}$
	CH ₄	C ₂ H ₆	C ₃ , HC	CH ₃ CHO	C ₂ H ₅ CHO	
Reduced Rh/SiO ₂						
373 K, 1 atm	0.025	0.139	-	-	0.016 (8.84) ^b	0.114
513 K, 1 atm	0.037	8.27	0.098	0.097	1.39 (14.1)	0.168
513 K, 10 atm	0.174	66.4	0.094	0.075	24.5 (26.8)	0.369
Oxidized Rh/SiO ₂						
373 K, 1 atm	0.012	0.075	-	-	0.025 (22.3)	0.333
Sulfided Rh/SiO ₂						
373 K, 1 atm	0.013	0.001	-	-	-	-
513 K, 1 atm	0.023	2.52	-	-	0.434 (14.6)	0.172
513 K, 10 atm	0.094	48.9	0.092	-	27.0 (35.5)	0.552

a: Ratio of the rate of product formation.

b: Selectivity to propionaldehyde (mol%).

to 513 K at 1 atm resulted in a significant increase in the rate of formation of ethane and propionaldehyde and a slight increase in the selectivity toward propionaldehyde. Increasing the reaction temperature also reduced the intensity and wavenumber of the linear CO and bridged CO bands, but increased the intensity of hydrocarbon bands. A wavenumber decrease for the linear CO and bridge CO has been attributed to a decrease in the dipole-dipole coupling between adsorbed CO [118] as a result of the dilution of adsorbed CO by adsorbed propionaldehyde and hydrocarbons.

Subsequent increases in pressure from 1 to 10 atm at 573 K further increased the rates of formation for methane, ethane, and propionaldehyde by factors of about 4.6, 8, and 17.5, respectively. The use of high pressures significantly enhanced the selectivity to propionaldehyde. The increases in pressure also caused a slight increase in the intensity of the linear CO band, the formation of the propionaldehyde band at 1730 cm^{-1} , and development of intense ethane bands at 2946 and 2890 cm^{-1} . No infrared evidence of CO adsorbed on Rh^+ ions was observed during the entire course of reaction studies on the reduced Rh/SiO_2 .

Figure 4.11 shows the infrared spectra as a function of time for ethylene hydroformylation on the oxidized Rh/SiO_2 catalyst at 373 K and 1 atm. Low reaction temperature and pressure were used to prevent the oxidized Rh surface from complete reduction. The rate of product formation corresponding to the IR spectra is listed in Table 4.1. Ethane, propionaldehyde, and methane were the major products. The infrared spectrum corresponding to the rate data showed the adsorbed CO band in the $2083\text{--}1800\text{ cm}^{-1}$ region. The 2083 cm^{-1} band is assigned to

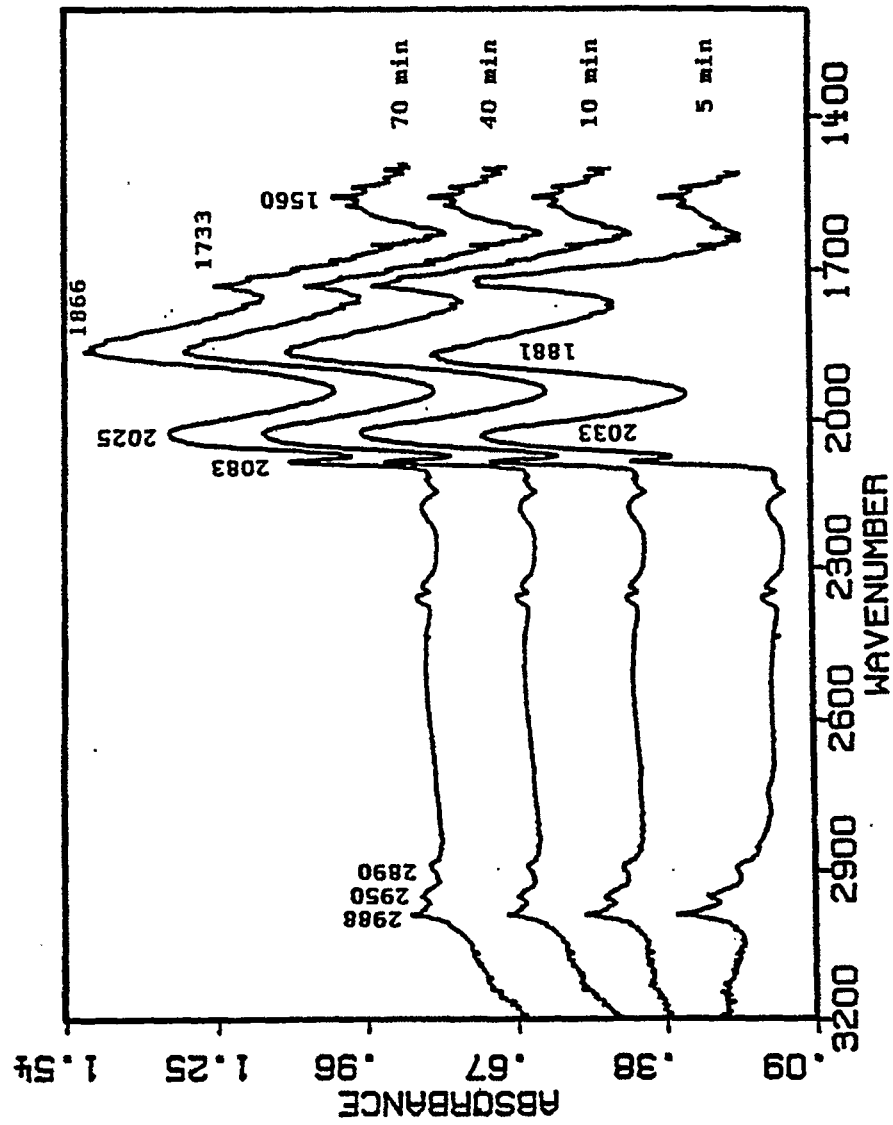


Figure 4.11 Ethylene Hydroformylation on the Oxidized Rh/SiO₂.

linearly adsorbed CO on Rh⁺ ions. The intensity of the band remained constant during the reactions. Repeated studies showed that the 2083 cm⁻¹ band evolved from the band in the 2096-2105 cm⁻¹ region which was assigned to the linear CO on the Rh⁺ site (shown in Figure 4.7). The bands at 2025 and 1881 cm⁻¹ are due to the linear CO and bridged CO on the reduced Rh crystallites. The presence of linear and bridged CO bands as well as the formation of CO₂ (at 2360 and 2340 cm⁻¹) on the oxidized Rh/SiO₂ indicates that the oxidized Rh surface was partially reduced during the reaction.

The 1560 cm⁻¹ band and the 1410 cm⁻¹ band (not shown in Figure 4.11) may be assigned to the bidentate of which oxygen atoms attach on a surface metal atom [89,117]. Studies on C₂ oxygenate synthesis over Rh/TiO₂ and Mn-Rh/SiO₂ have suggested that the bidentate species is the reaction intermediate for the formation of C₂ oxygenates [89]. In contrast, Fukushima et al. [93] have proposed that the bidentate species is formed from the spill-over of an adsorbed acetyl species on the Rh metal to the oxide. The propionaldehyde band at 1733 cm⁻¹ and the ethane bands at 2950-2890 cm⁻¹ decreased slightly in intensity with reaction time while the bidentate band at 1560 cm⁻¹ remained constant during the reaction. The propionaldehyde band observed on the oxidized Rh/SiO₂ is significantly more intense than that on the reduced Rh/SiO₂ (shown in Figure 4.10). The results are consistent with the considerably high propionaldehyde selectivity observed on the oxidized Rh/SiO₂ compared to the reduced Rh/SiO₂.

Figure 4.12 shows the infrared spectra of ethylene hydroformylation on the sulfided Rh/SiO₂. The rate of product formation is listed in Table 4.1. At 373 K and 1 atm, the linear CO at

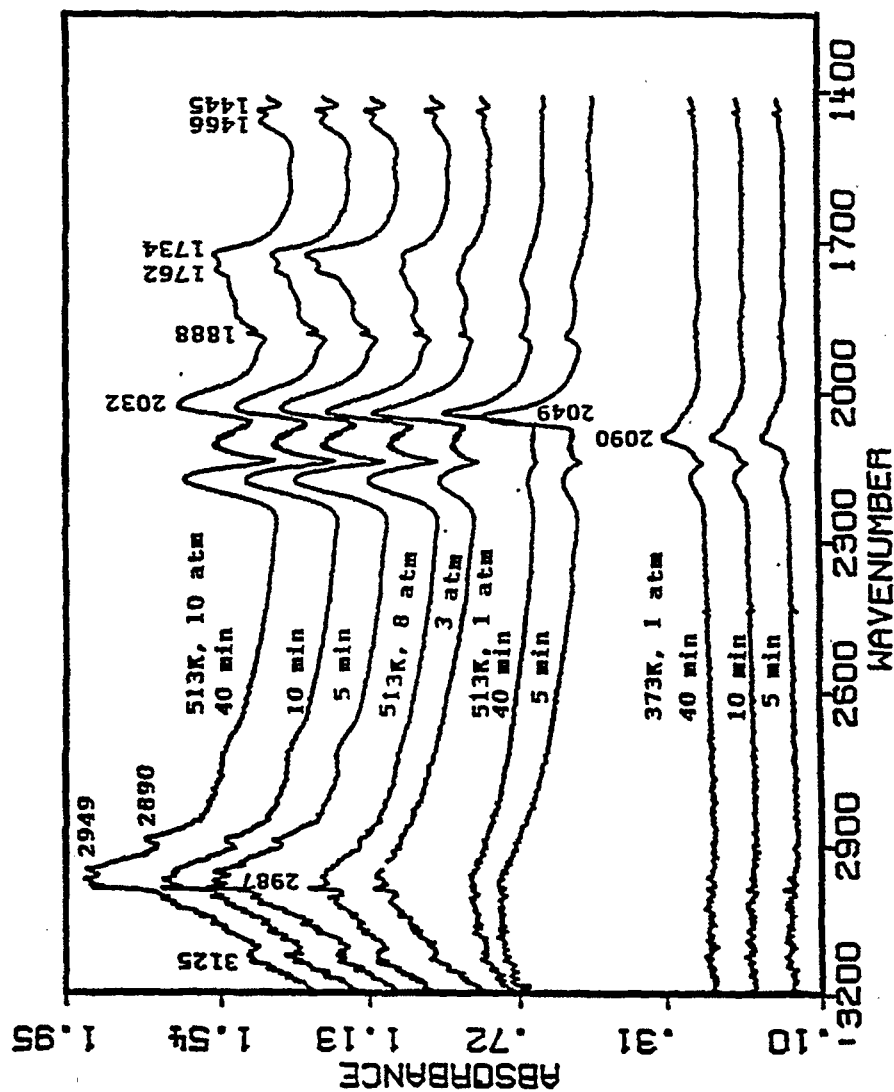


Figure 4.12 Ethylene Hydroformylation on the Sulfided Rh/SiO₂.

2090 cm^{-1} was the only adsorbed CO on the catalyst; methane and ethane were the observed products. Increasing the reaction temperature from 373 to 513 K at 1 atm resulted in the formation of propionaldehyde and an increase in the rate of formation of hydrocarbons. The increase in temperature also caused an increase in the intensity of the linear CO band and emergence of weak propionaldehyde and hydrocarbon bands. Subsequent increases in reaction pressure from 1 to 10 atm at 513 K slightly increased the intensities of the linear CO and further enhanced the intensity of the propionaldehyde and hydrocarbon bands; the increasing pressure also increased the formation rates of methane, ethane, and propionaldehyde by a factor of 4, 19.5, and 62.8, respectively. High pressure greatly enhanced the rate and selectivity for the formation of propionaldehyde.

4.4 Discussion

4.4.1 Characterization of the Rh Surface by Infrared Spectroscopy of CO Adsorption

The types of CO adsorbed on the Rh catalysts are very sensitive to the structure and chemical environment of the Rh surface. It has been well established that the reduced Rh crystallite surface chemisorb CO as linear and bridge CO species; the oxidized Rh surface contains isolated Rh^+ sites which adsorb CO as gem-dicarbonyl [119-125]. The sulfided Rh surface also possesses isolated Rh sites which have been suggested to carry positive charges; these sites chemisorb CO as linear CO or gem-dicarbonyl [112].

Three types of adsorbed CO species including linear CO, bridge CO, and gem-dicarbonyl were clearly observed from the spectra of CO adsorbed on the reduced Rh/SiO₂ catalyst, as shown in Figure 4.2. The

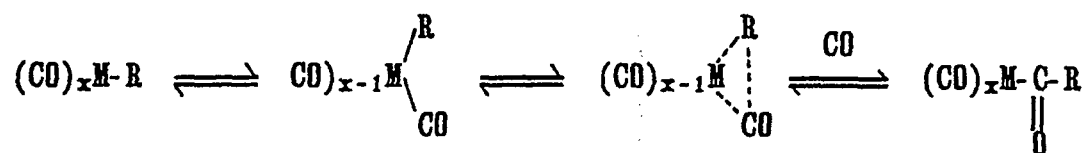
results indicate that the surface of the reduced Rh/SiO₂ contains both reduced Rh crystallite and isolated Rh⁺ sites. XPS studies revealed that the surface of reduced Rh/SiO₂ prior to CO adsorption contains primarily the reduced Rh⁰ atoms. The observation of gem-dicarbonyl suggests that CO adsorption led to the formation of isolated Rh⁺ sites on the reduced Rh/SiO₂. The formation of Rh⁺(CO)₂ from adsorption of CO on Rh⁰ sites has been found to involve isolated OH groups. The process can be reversed by hydrogen treatment [144-146].

XPS studies (shown in Figure 4.1) have shown that oxidation of the reduced Rh/SiO₂ at 513 K produced the oxidized Rh/SiO₂ whose surface contains primarily Rh⁺ ions. CO adsorption on the oxidized Rh/SiO₂ produced linear CO and gem-dicarbonyl adsorbed on the isolated Rh⁺ ions. Increasing CO pressures led to formation of bridge CO adsorbed on Rh crystallites as well as an unknown CO species. The formation of bridge CO indicates that part of the oxidized Rh surface was reduced during CO adsorption.

4.4.2 CO Insertion

The metal carbonyl hydrides play a central role in the catalytic chemistry of CO insertion [47]. Metal carbonyl hydride such as HCo(CO)₄ can protonate methanol resulting in the formation of methyl cobalt intermediates and the subsequent migratory CO insertion leading to the formation of ethanol. The labile nature of the M-H bond in the metal carbonyl hydride also permits olefin insertion leading to the formation of an alkyl metal intermediate; the following migration of

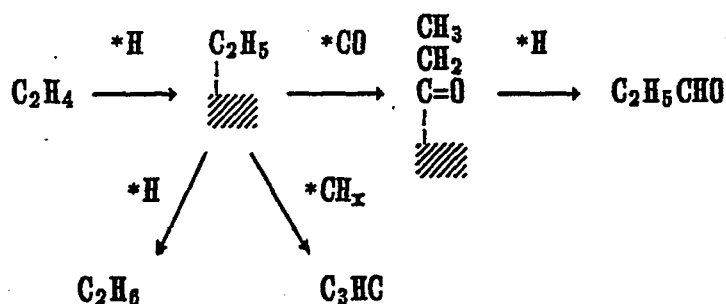
the alkyl group to the carbon of the CO ligand (also known as the migratory CO insertion) resulted in the formation of an acyl intermediates [45,46].



R: alkyl group M: metal

In the process of the migratory CO insertion, the metal center of the carbonyl species maintains its oxidation state of +1 [46-50]. The reaction has been observed for all group VIII metal carbonyls and complexes [48].

The apparent analogy between the well-defined organometallic reaction steps and the elementary step on the heterogeneous catalyst surface has been used as a basis for the development of CO insertion mechanism on the surface of supported Rh catalysts [39,54,55]. The suggested pathway for the CO insertion in ethylene hydroformylation over supported Rh catalysts is presented as following [39,57].



The formation of propionaldehyde involves three major steps: hydrogenation of adsorbed C_2H_4 to form adsorbed ethyl species, insertion of adsorbed CO into $^*\text{C}_2\text{H}_5$ to form adsorbed acyl species, and

then hydrogenation to produce propionaldehyde. The occurrence of 66
migratory CO insertion on the metal center with an oxidation state of
+1 in organometallic chemistry suggests that CO insertion may also take
place on the Rh^+ site on the supported Rh catalyst [40]. The mechanism
involving CO insertion on the Rh^+ sites has been proposed on the basis
of the following observations: (i) pre-oxidation of Rh foil increased
the initial rates and selectivity for the formation of oxygenates from
CO hydrogenation and ethylene addition [58], and (ii) the catalysts
containing Rh^+ ions exhibited higher rates for C_2 oxygenate synthesis
and ethylene hydroformylation than those containing Rh^0 [58,59,64,65].
On the contrary, lack of correlation of the activity for C_2 oxygenate
synthesis and ethylene hydroformylation to the Rh^+ concentration has
been reported by a number of studies [66-67]. It should be noted that
the sites for C_2 oxygenate synthesis include CO dissociation,
hydrogenation, and CO insertion sites while ethylene hydroformylation
occurs on hydrogenation and CO insertion sites. The catalysts which
are active for ethylene hydroformylation generally show high
selectivity for C_2 oxygenate synthesis [39,55,68,57].

The correlation between the formation of propionaldehyde and
consumption of specific forms of adsorbed CO should permit unequivocal
identification of the forms of CO involved in the CO insertion leading
to the formation of propionaldehyde. The direct correlation between
the propionaldehyde production and the linear CO consumption observed
in Figure 4.6 and 4.8 indicated that linear CO adsorbed on the Rh^0 site
participates in CO insertion on the reduced Rh/SiO_2 ; linear CO adsorbed
on the Rh^+ site takes part in CO insertion on the oxidized Rh/SiO_2 .
Other adsorbed CO species including gem-dicarbonyl and bridge CO serve

as spectator species which are not involved in the reaction.

Comparison of the rate of growth of propionaldehyde bands in Figures 4.6 and 4.7 shows that the oxidized Rh/SiO₂ is more active for catalyzing the formation of propionaldehyde than the reduced Rh/SiO₂, suggesting that Rh⁺ sites are more active for CO insertion than Rh⁰ sites.

The dominant CO species observed during ethylene hydroformylation on the reduced Rh/SiO₂ are the linear CO and bridge CO adsorbed on the Rh⁰ crystallite sites. High rate of ethane formation and low rate of propionaldehyde formation on the reduced Rh/SiO₂ as compared to the oxidized and sulfided Rh/SiO₂ catalyst can be attributed to the high hydrogenation activity of Rh crystallite surface. The variation of reaction temperatures and pressures from 373 K and 1 atm to 513 K and 10 atm has little influence on the adsorbed CO. Comparison of the wavenumbers of linear CO in Figures 4.6 and 4.10 shows that the linear CO under hydroformylation conditions exhibits lower wavenumbers than those observed under CO adsorption. This is primarily due to the dilution of adsorbed CO by adsorbed reactants and products. The dilution effect can be further confirmed by the observation that the decreasing wavenumber and intensity of the linear CO band is accompanied by the growing hydrocarbon and propionaldehyde bands shown in Figure 4.10.

The linear CO on the Rh⁺ sites as well the linear CO and bridge CO on the Rh⁰ sites are the major adsorbed CO species during ethylene hydroformylation on the oxidized Rh/SiO₂. The results indicate that both Rh⁺ and Rh⁰ sites are present on the oxidized Rh/SiO₂ during the reaction. Due to the lack of information on the number of active sites

on the reduced Rh and oxidized Rh catalysts, the direct comparison 68
of the activity of these two catalysts is not possible. However, the
intensity of the linear and bridge CO may be used for a rough
comparison of the amount of CO adsorbed on the catalyst assuming the
extinction coefficient of the adsorbed CO on Rh⁰ sites is similar for
both the oxidized and reduced Rh/SiO₂. The intensity of linear CO and
bridge CO on the Rh⁰ sites is greater on the oxidized Rh/SiO₂ than on
the reduced Rh/SiO₂ indicating that the oxidized Rh/SiO₂ has a greater
amount of Rh⁰ sites than the reduced Rh/SiO₂. In spite of the surface
of the oxidized Rh/SiO₂ containing considerable amount of Rh⁰ sites,
the oxidized Rh/SiO₂ catalyst exhibited higher selectivity to
propionaldehyde than the reduced Rh/SiO₂ in steady-state ethylene
hydroformylation. The high activity and selectivity of the oxidized
Rh/SiO₂ appears to be due to the presence of Rh⁺ sites on the oxidized
Rh/SiO₂. Our results are in good agreement with previous reports for
the catalysts containing Rh⁺ sites which exhibited high selectivity for
C₂ oxygenate synthesis and ethylene hydroformylation [39,40,58,65].

The different conclusions drawn from various studies on the
active site for CO insertion can be reconciled by results of the
present study. Results of this study have shown that both single Rh⁰
atoms and single Rh⁺ ions are active for CO insertion. The observation
of Rh⁰ catalyzing CO insertion is in good agreement with previously
observed high C₂ oxygenate synthesis and hydroformylation activities
for LaRhO₃ and Rh/V₂O₃ which contain only Rh⁰ sites [66-68]. It is
likely that the Rh⁰ on the surface of these catalysts is also in single
atom state.

The important role of the single Rh atom site in CO insertion can be demonstrated by the high selectivity and activity of the sulfided Rh/SiO₂ for ethylene hydroformylation. The bridge CO sites can be blocked by adsorbed sulfur [55,74] resulting in the formation of isolated Rh sites which give rise to only linear CO as shown in Figure 4.5. Comparison of the rate data and IR data for the reduced and sulfided Rh/SiO₂ catalysts shows that the rate, selectivity, and infrared intensity for propionaldehyde are greater on the sulfided Rh than on the reduced Rh at 513 K and 10 atm. Adsorbed sulfur also shifts the wavenumber of linear CO to higher wavenumber indicating that adsorbed sulfur makes the neighboring Rh atom more electropositive. In spite of its high activity and selectivity for ethylene hydroformylation, the sulfided Rh/SiO₂ exhibited little reactivity for the reaction of C₂H₄ and H₂ with adsorbed CO at 301 K as a result of the inhibition of C₂H₄/H₂ adsorption brought about by adsorbed sulfur.

Additives including Ag [85], Zn [83,84], and Fe [86] have been found to block bridge CO sites. The blockage of bridge CO sites by these additives increases the ratio of the linear CO to bridge CO sites resulting in enhancement of CO insertion selectivity. Ponc and coworkers [66] have suggested that the blocking of the Rh surface by supports such as V₂O₃ could result in the suppression of hydrocarbon formation and the enhancement of the selectivity for C₂ oxygenate synthesis. In addition to the site blockage effect of additives, other possible effects of additives on C₂ oxygenate synthesis include the following: stabilization of Rhⁿ⁺ sites, activation of CO by oxophilic

additives (Mn and Zr), stabilization of the oxygenated intermediates ⁷⁰
[11,64,92].

Although the reduced, oxidized, and sulfided Rh/SiO₂ catalysts exhibit CO insertion activity, the selectivity of these catalysts for the CO insertion reaction remain significantly lower than that of Rh carbonyls and complexes which have long been used for commercial hydroformylation and carbonylation [46-49]. An understanding of the role of CO insertion sites in hydrogenation, the side reaction of hydroformylation, is essential for the improvement of selectivity of heterogeneously supported-metal catalysts for the CO insertion related reactions.

4.5 Conclusions

The linear CO species adsorbed on both single Rh⁰ atom and Rh⁺ ion sites have been found to participate in CO insertion leading to the formation of propionaldehyde from C₂H₄ and H₂. The linear CO on the Rh⁺ site of the oxidized Rh/SiO₂ appears to be more active for CO insertion than those on the reduced Rh⁰ site of the reduced Rh/SiO₂. These results show that both single Rh⁰ atom and Rh⁺ ion sites serve as active sites for CO insertion. The dominant CO species in ethylene hydroformylation are the linear CO and bridge CO on the Rh⁰ crystallite surface of the reduced Rh/SiO₂, linear CO on the Rh⁺ sites as well as the linear CO and bridge CO on the Rh⁰ crystallite surface of the oxidized Rh/SiO₂, and the linear CO on the sulfided Rh/SiO₂. The oxidized Rh/SiO₂ exhibited higher rates and selectivities for the formation of propionaldehyde than the reduced Rh/SiO₂ at 313 K and 1 atm; under high pressure and temperature (513 K and 10 atm) the

sulfided Rh/SiO₂ exhibited higher rates and selectivities for the 71
formation of propionaldehyde than the reduced Rh/SiO₂. The difference
in activity and selectivity of these catalysts for ethylene
hydroformylation can be attributed to the different surface states of
Rh on these catalysts. Both electronic state and geometric structure
(size of ensembles) of surface Rh atoms play important roles in
determining CO insertion activity and selectivity.

CHAPTER V

HIGHER OXYGENATE SYNTHESIS FROM REACTION OF ETHYLENE WITH
SYNGAS ON Ni/SiO₂ AND SULFIDED Ni/SiO₂

5.1 Introduction

The reaction of ethylene with syngas has been used as a probe reaction for investigating the mechanism of the Fischer-Tropsch (F-T) synthesis and the activity of F-T catalysts for catalyzing the specific reaction steps [58,74,94]. The added ethylene may undergo various specific reactions: (i) hydrogenation, (ii) chain incorporation, and (iii) CO insertion leading to the formation of ethane, C₃ hydrocarbons, and propionaldehyde, respectively. The selectivity of F-T catalysts has been shown to depend on their capabilities for these specific reactions [58,94]. In general, a catalyst which exhibits a strong CO insertion activity is active for producing C₂ oxygenates in the F-T synthesis. The catalysts including Rh, Ru, Co, Fe, and Mo have been shown to exhibit the activity for CO insertion [36-44].

Ni is known to be an active catalyst for the F-T synthesis [8,57]. Due to its high methanation activity and selectivity, the catalytic capabilities of Ni catalyst for other syngas related reactions have been overlooked. Our recent study found that Ni/SiO₂, a methanation catalyst, exhibits CO insertion activity; its activity for CO insertion is comparable to that of Rh which is known to be the most

active for CO insertion; and sulfur poisoning of both Ni/SiO₂ and Rh/SiO₂ catalysts leads to enhancement of ethylene hydroformylation in reaction of ethylene with syngas [74].

The present study was aimed at developing a better understanding of the CO insertion reaction on Ni/SiO₂ catalysts. In situ infrared spectroscopy studies of CO/H₂ and C₂H₄/CO/H₂ reactions were undertaken. The enhance of ethylene hydroformylation over Ni/SiO₂ through sulfur promotion was studied.

5.2. Experimental

5.2.1 Catalyst Preparation and Characterization

14.4 wt% Ni/SiO₂ was prepared by impregnation of SiO₂ using Ni(NO₃)₂ · 6H₂O. The procedure of the catalyst preparation has been described in Chapter III. The Ni crystalline size was determined to be 108 Å by X-ray diffraction line-broadening. The catalysts for the study were ground to a fine powder and pressed into a disk with 25 mg. The catalyst was reduced in H₂ flow at 513 K for 1 hr before reaction studies. Sulfidation of Ni/SiO₂ was performed by passing 1000 ppm H₂S in H₂ through the IR cell at 513 K for 1 hr.

5.2.2 Experimental Procedure

CO/H₂ and C₂H₄/CO/H₂ reactions on Ni/SiO₂ were studied in the IR cell at 513 K and 1-30 atm. IR spectra were taken under steady-state (S.S.) flow condition and closed system (C.S.). Steady-state IR spectra were recorded after reactant flow was maintained at steady state for 20 min. Subsequent to recording each S.S. IR spectrum, the composition of reactor effluent was analyzed by GC. The reaction pressure was raised by shutting off the reactor effluent and maintaining constant inlet flow rate. Once the desired pressure was

reached, the reactor inlet was closed to maintain the pressure at constant for 5 min prior to recording C.S. IR spectrum.

5.3 Results and Discussion

5.3.1 CO/H₂ Reaction on Ni/SiO₂

IR spectra of CO/H₂ reaction on Ni/SiO₂ at 513 K, 1-20 atm are shown in Figure 5.1. Table 5.1 shows the rates of CO conversion and product distribution corresponding to each IR spectrum taken under steady-state (S.S.) condition. Two major bands were observed for CO/H₂ reaction at 1 atm: linearly adsorbed CO at 2046 cm⁻¹ and bridge-bonded CO at 1890 cm⁻¹. Bands around 2927 cm⁻¹ can be assigned to the C-H stretching vibration of hydrocarbon species. Methane was identified to be the major product while no oxygenates were observed under these conditions. As the reaction pressure was slowly increased to 10 atm, a band at 2055 cm⁻¹ became prominent whereas the band at 2046 cm⁻¹ was attenuated. The increases in reaction pressure also led to marked decreases in the rate of CO conversion. Shutting off the reaction inflow and outflow and maintaining the reaction pressure at 10 atm led to further growth of the band 2055 cm⁻¹. This band corresponds to the wavenumber of gaseous Ni(CO)₄ [114]. Resuming the S.S. flow condition and keeping in the reaction pressure at 10 atm resulted in a marked decrease in the intensity of both Ni(CO)₄ and bridge CO band. The band at 2055 cm⁻¹ was also observed in the gas sample collected from the effluent of IR reactor cell. These observations indicate that Ni(CO)₄ produce from carbonylation of Ni surface was transported with reactant stream from the catalyst to the reactor effluent.

Increasing reaction pressure from 10 to 20 atm and maintaining the steady-state reaction flow resulted in reduction of all the

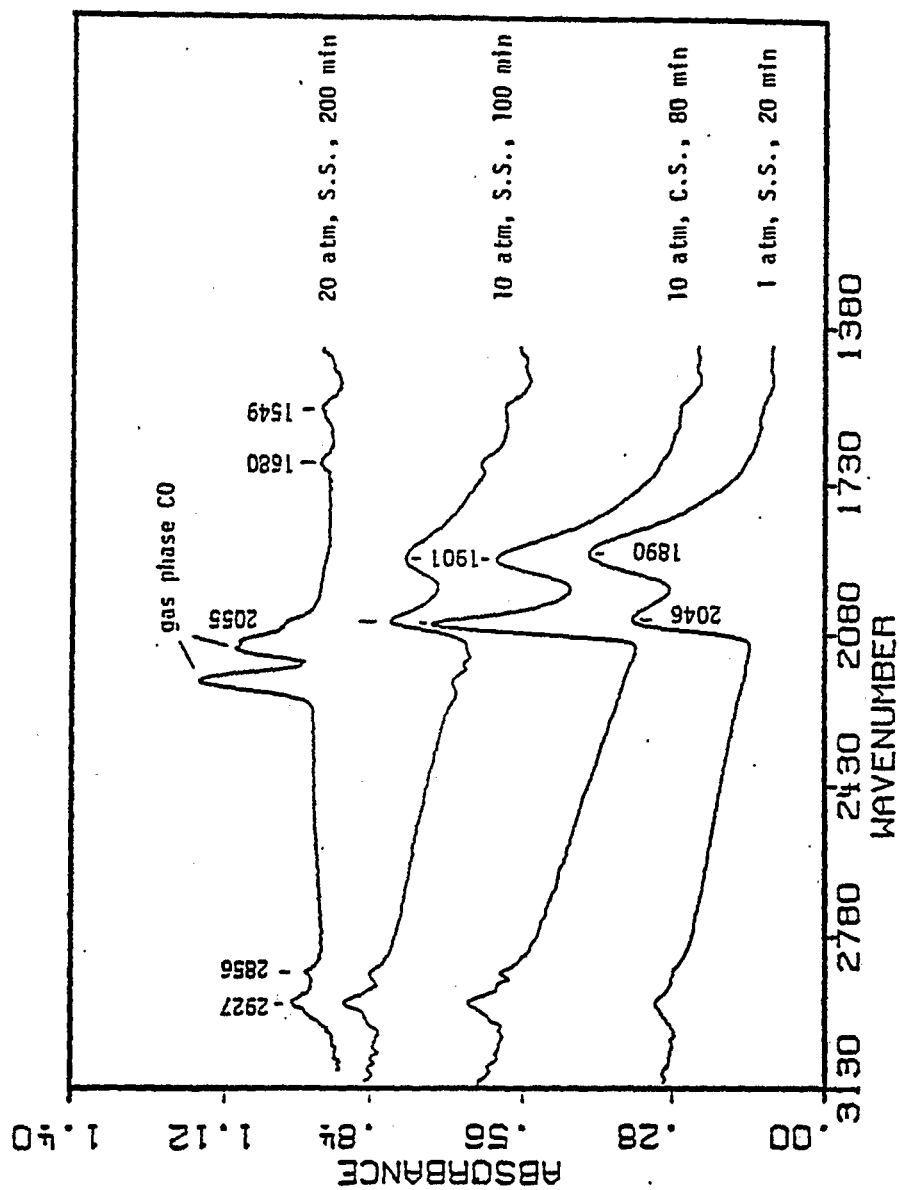


Figure 5.1 Infrared Spectra of CO/H₂ Reaction on Ni/SiO₂: S.S. (steady state): The spectrum was taken while the reactant flow was maintained at steady state. C.S. (closed system): The spectrum was taken while both the inlet and outlet of IR reactor was closed.

Table 5.1 Product Selectivity of CO/H₂ Reaction on Ni/SiO₂

Pressure (atm)	Overall Rate (mol/g-hr)	Selectivity (mol%)			
		CH ₃	C ₂ H ₄	C ₂ H ₆	C ₃ H ₈ C ₄ H ₁₀
1	0.22	65.2 (0.099) ^a	17.1	8.1	6.2 2.8
10	0.36	30.9 (0.064)	43.0	22.9	3.2 0.0
20	0.14	26.0 (0.021)	60.3	13.7	0.0 0.0

Reaction Temperature: 513 K Fresh Ni/SiO₂ : 14.4%
CO:H₂ = 1:1 Used Ni/SiO₂ : 6.9%

^a : Value in parenthesis is the rate of methane formation (mol/Kg-hr).

adsorbed CO and $\text{Ni}(\text{CO})_4$ bands. This increase in the reaction pressure also led to the decrease in CO hydrogenation activity (see Table 5.1). Chemical analysis of the Ni catalysts also revealed that the Ni loading decreased from 14.4 % (fresh catalyst) to 6.9 % during the entire period of CO hydrogenation study. These results suggest that part of the Ni atoms for CO hydrogenation have been removed from Ni/SiO₂ by carbonylation. Carbonyl formation can be one of the major causes for deactivation of Ni-based catalysts for the F-T reaction [8,114].

5.3.2 C₂H₄/CO/H₂ Reaction on Ni/SiO₂

A fresh Ni/SiO₂ was used for IR studies of C₂H₄/CO/H₂ reaction. Figure 5.2 shows IR spectra of C₂H₄/CO/H₂ reaction. Gaseous ethylene bands appeared around 1915, 1859, 1466, and 1414 cm⁻¹. Comparison of IR spectra of C₂H₄/CO/H₂ with those of CO/H₂ (Figure 5.1) shows that the addition of ethylene to syngas caused a downward shift of both linear and bridge CO bands at 1 atm. The downward shift of CO bands may be attributed to the dilution of the adsorbed CO layer caused by adsorbed ethylene species [118]. As shown in Table 5.2, the major hydrocarbon products of the reaction are methane and ethane. High ethane formation rate indicates that the majority of ethane are formed from ethylene hydrogenation. Hydrogenolysis of C₂ hydrocarbons appears to occur to a significant extent as indicated by high methane formation rate in the C₂H₄/CO/H₂ reaction compared with that in the CO/H₂ reaction. Appreciable amount of propionaldehyde and 1-propanol was also observed at the pressure above 1 atm. As the pressure was increased to 10 atm, the bands at 1721 and 1678 cm⁻¹ began to appear. The former corresponds to adsorbed propionaldehyde. The band at 1678

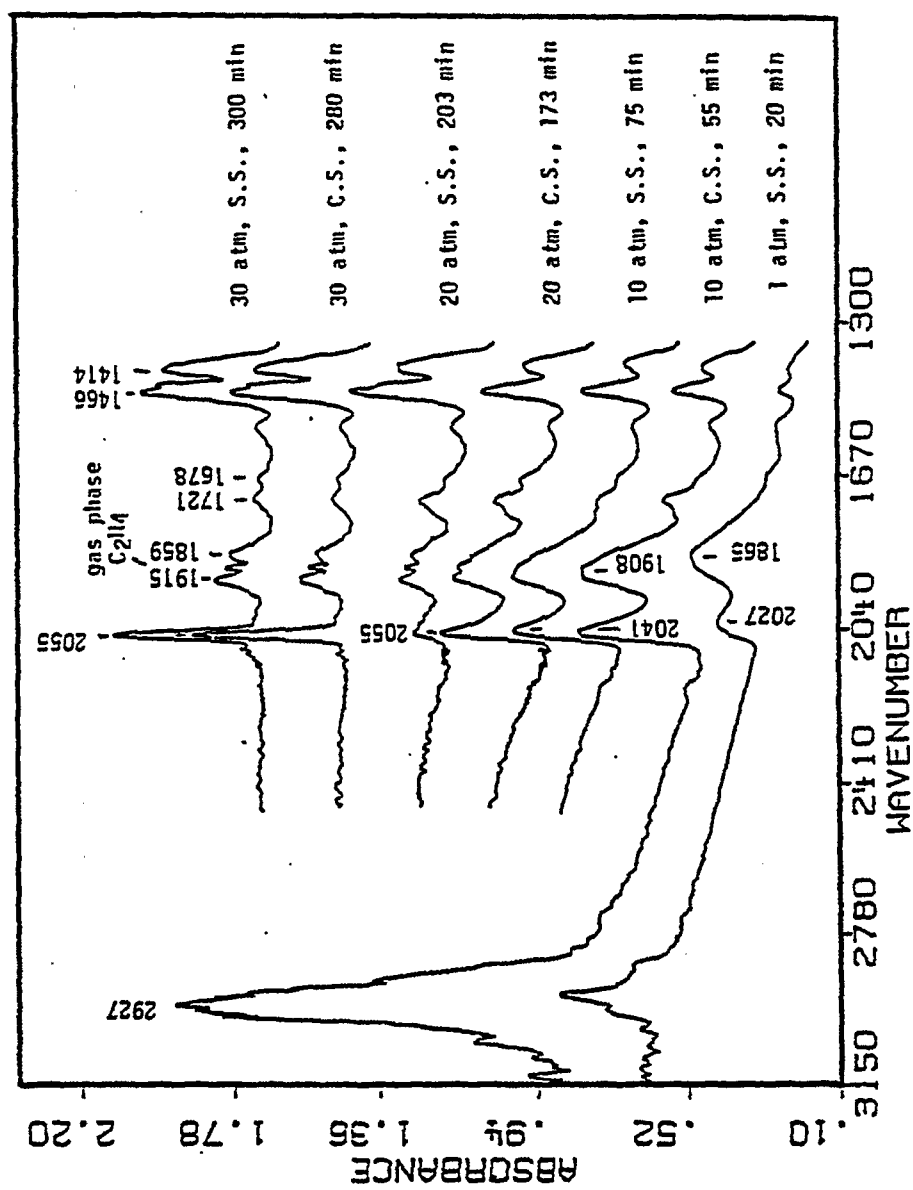


Figure 5.2 Infrared Spectra of $C_2H_4/CO/H_2$ Reaction on Ni/SiO_2 .

Table 5.2 Product Selectivity of $C_2H_4/CO/H_2$ Reaction on S-Ni/SiO₂ and Ni/SiO₂

Catalyst/Prection Condition	Selectivity (mol%)			
	CH ₄	C ₂ H ₆	C ₃ H ₈	C ₂ H ₅ CHO C ₃ H ₇ OH
Ni/SiO₂^a				
513 K, 1 atm	2.0	92.9 (36.6) ^c	2.5	2.4 (0.96) ^c 3.8
513 K, 10 atm	1.3	87.8 (62.3)	1.5	8.6 (6.1) 0.8
513 K, 20 atm	1.1	89.9 (51.5)	1.3	7.5 (4.3) 0.2
513 K, 30 atm	0.6	87.4 (48.8)	0.6	11.1 (6.2) 0.3
S-Ni/SiO₂^b				
513 K, 1 atm	4.1	83.4 (0.6)	0.2	8.5 (0.06) 3.8
513 K, 10 atm	0.0	66.3 (13.6)	1.4	31.1 (6.4) 1.2
513 K, 20 atm	0.2	64.9 (12.9)	0.2	33.9 (6.7) 0.8
513 K, 30 atm	0.2	58.8 (14.5)	0.6	40.3 (9.9) 0.1

a : Fresh Ni/SiO₂: 14.4 wt%, Used Ni/SiO₂: 7.2 wt%b : Fresh Ni/SiO₂: 14.3 wt%, Used Ni/SiO₂: 6 wt%

c : Value in parathesis is the rate of formation (mol/Kg-hr).

cm⁻¹ may be assigned to adsorbed acyl species (Ni(CO)C₂H₅) which is 80 analogous to acyl-rhodium species [36,38]. The presence of adsorbed acyl species suggests that the propionaldehyde may be formed via CO insertion pathway on Ni.

Comparison of the IR spectra as well as product formation rate in Figure 5.2 and Table 5.2 shows several interesting features of pressure effect on the IR spectra and the rate of product formation. Increases in total reaction pressure led to (i) increases in the intensity of Ni(CO)₄ band under C.S. condition, (ii) increases in the intensity of both linear and bridge CO for the pressure from 1 to 10 atm and decreases in intensity of both adsorbed CO for the pressure above 10 atm, (iii) increases in the rate of formation of propionaldehyde and 1-propanol, (iv) decreases in the rate of ethane formation from 10 to 30 atm, and (v) decreases in the rate of methane formation. It is important to point out that the Ni(CO)₄ band observed under S.S. condition is always smaller than that of Ni(CO)₄ observed under C.S. condition. This is due to the removal of gaseous Ni(CO)₄ by the steady-state reactant flow. The removal of Ni from the Ni/SiO₂ is also evidenced by the decrease of Ni loading from 14.4 % to 7.2 % during C₂H₄/CO/H₂ study.

Carbonylation of Ni/SiO₂ which was observed in CO hydrogenation was also observed in reaction of ethylene with syngas as indicated by the formation of Ni(CO)₄ at high pressure. Comparison of transmission electron microscopy of both fresh and used catalysts shows no obvious difference in the size of Ni particle. Carbonylation of Ni/SiO₂ under reaction conditions, especially at high pressures, led to the removal of the reduced Ni atoms resulting in decreases in rates of CO

hydrogenation and ethylene hydrogenation as well as in the IR intensity of adsorbed CO band.

At the end of both CO/H₂ and C₂H₄/CO/H₂ reaction studies, almost 50% of Ni was removed from the Ni/SiO₂ catalysts and the catalysts exhibited very weak bands of adsorbed CO indicating that part of the Ni remains on the Ni/SiO₂ may not be in the reduced state. This may be due to incomplete reduction of the Ni catalyst at the reduction temperature of 673 K. It has been shown that reduction of Ni oxide to the zero-valent Ni is the required step for the carbonylation of Ni oxides to Ni(CO)₄ [48]. Infrared studies of CO adsorption on unreduced Ni catalysts revealed that carbonylation did not occur on the unreduced catalysts. Although the intensity of the Ni(CO)₄ band is in parallel with the rate of formation of propionaldehyde, Ni(CO)₄ is well known to be inactive for homogeneous hydroformylation [48]. The active sites for the formation of propionaldehyde appear to be on the surface of the Ni/SiO₂ catalysts.

In contrast to C₂ oxygenate synthesis catalysts such as Rh [39,57], Ni/SiO₂, which exhibits strong methanation activity during CO/H₂ reaction, is active for catalyzing the formation of propionaldehyde in the reaction of ethylene with syngas. The reason for the absence of a correlation in the oxygenate selectivity between CO/H₂ and C₂H₄/CO/H₂ reactions on the Ni/SiO₂ remains unclear.

5.3.3 Sulfur Effect on Ethylene Hydroformylation

Table 5.2 shows comparison of the reaction rate and product selectivity for ethylene hydroformylation over sulfided Ni/SiO₂ (S-Ni/SiO₂) and Ni/SiO₂. The data for both catalysts were taken at the same interval since the onset of the reaction. Sulfidation led to an

increase in propionaldehyde selectivity by a factor of 3-4 at 513 K ⁸² and 1-30 atm. Such an increase in selectivity to propionaldehyde can be attributed to the reduction in the rate of ethylene hydrogenation and the enhancement in the rate of ethylene hydroformylation at pressures from 10 to 30 atm brought about by adsorbed sulfur. While adsorbed sulfur is known to poison olefin hydrogenation [97], it appears to be effective in promoting ethylene hydroformylation.

As the reaction pressure increased from 1 to 30 atm, the propionaldehyde selectivity increased on both catalysts. IR spectra taken for the reaction on S-Ni/SiO₂ corresponding to the product selectivity and the rate of product formation listed in Table 5.2 are given in Figure 5.3. The major bands observed for the reaction at 1 atm are linearly adsorbed CO at 2066 cm⁻¹ and hydrocarbon bands at 2800-3050 cm⁻¹. The increase in the reaction pressure led to (i) a growth of gaseous ethylene bands and hydrocarbon bands due to product of hydrocarbons, (ii) a shift of the 2066 cm⁻¹ band to 2054-2057 cm⁻¹ which is corresponding to Ni(CO)₄, and (iii) an emerge of a propionaldehyde band at 1728 cm⁻¹ and an acyl species at 1678 cm⁻¹. The absence of linearly adsorbed CO band at high pressures appears to be due to overlapping by the strong Ni(CO)₄ band. Chemical analysis of the catalysts (by Galbraith Lab.) show that the Ni loading decreased from 14.4 % (fresh catalyst) to 2.9 % during the entire period of the hydroformylation study.

The loss of the Ni is significantly greater for the S-Ni/SiO₂ as compared with Ni loss for the reaction on Ni/SiO₂ for the same reaction condition. The great loss of Ni from S-Ni/SiO₂ may be due to the promoting effect of sulfur on the formation of Ni(CO)₄. Qudar [97]

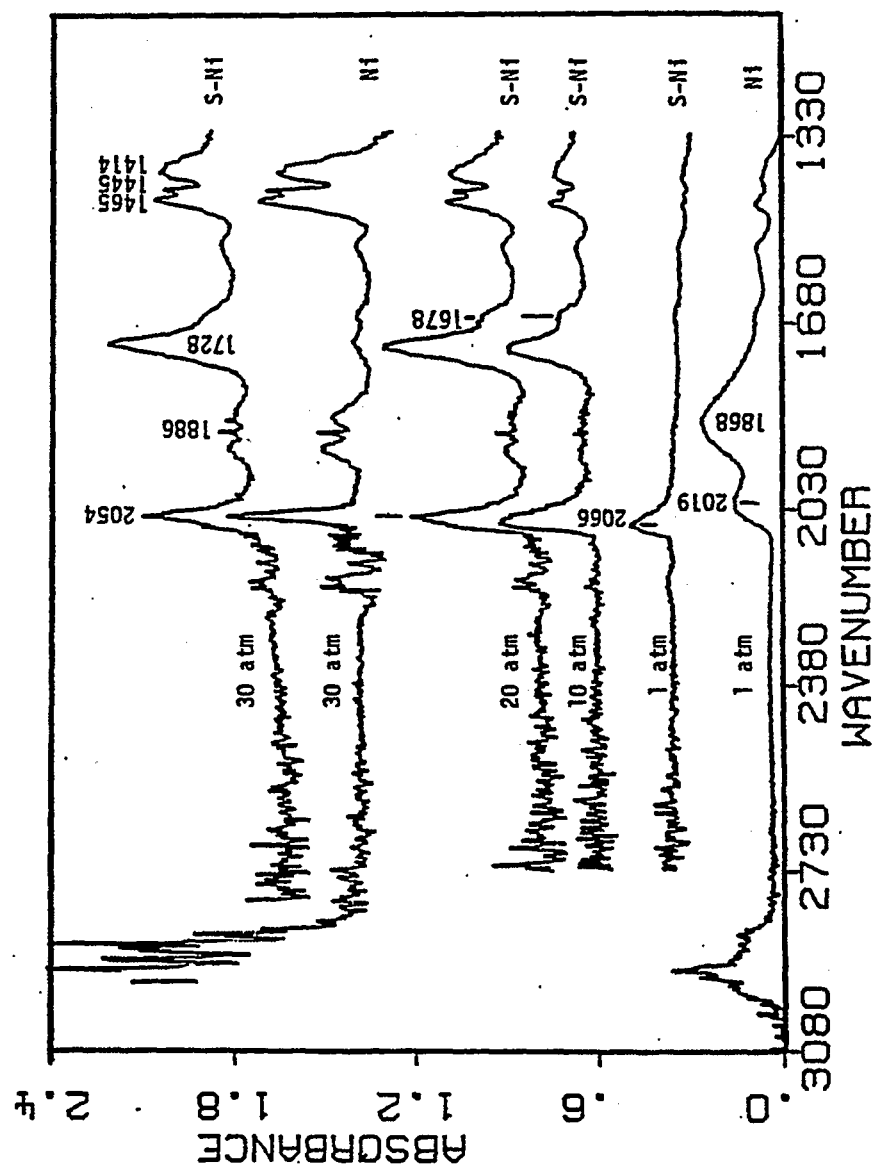


Figure 5.3 Infrared Spectra of $C_2H_4/CO/H_2$ Reaction on S-Ni/SiO₂.

has suggested that adsorbed sulfur could cause a weakening of the Ni ⁸⁴ substrate and the CO-substrate bond; weakly adsorbed CO would be a better candidate for the carbonyl formation than the more strongly bonded CO.

Figure 5.3 also includes IR spectra of ethylene hydroformylation on Ni/SiO₂ at 1 and 30 atm. Comparison of IR spectra before and after sulfidation at 1 atm shows that sulfidation of the catalyst led to the suppression of the bridge CO band and the shift of the linear CO to higher wavenumbers. The loss of bridge CO site indicates that the pair-surface Ni atoms has been disrupted by adsorbed sulfur resulting in the formation of isolated Ni atom; the shift of linear CO band to higher numbers may be attributed to the weakening of metal-CO bond as a result of decreases in back-donation of electron from sulfided Ni surface to antibonding of CO molecules. However, such a shift was not obvious for the reaction at 30 atm since the prominent Ni(CO)₄ band may cover the weak band of adsorbed CO.

Comparison of the rate and IR data at 30 atm for S-Ni and Ni shows that the intensity of adsorbed propionaldehyde and acyl bands and the rate of propionaldehyde formation were greater for S-Ni/SiO₂ than for Ni/SiO₂. The results clearly indicate that adsorbed sulfur serves as a promoter to enhance propionaldehyde formation on the Ni/SiO₂ catalyst. The observations of (i) lack of the bridge CO and higher hydroformylation rate on the Ni/SiO₂ at high reaction pressures and (ii) the suppression of the bridge CO sites and enhancement of hydroformylation brought about by adsorbed sulfur indicate that the isolated Ni atom site may be responsible for the reaction.

Due to the ease of the formation of Ni(CO)_4 from sulfided Ni/SiO_2 , the pure sulfided Ni catalyst is not suitable for the commercial hydroformylation. Further modification of the catalyst by addition of promoters to suppress the carbonyl formation and hydrogenation is required for the successful development of a Ni-based catalyst for commercial hydroformylation processes.

5.4 Conclusions

Ni/SiO_2 shows to exhibit CO insertion activity. In situ infrared studies of CO/H_2 and $\text{C}_2\text{H}_4/\text{CO/H}_2$ reactions on Ni/SiO_2 show that carbonylation of Ni/SiO_2 to Ni(CO)_4 leads to an inhibition of methanation in CO hydrogenation but an enhancement of formation of propionaldehyde in the $\text{C}_2\text{H}_4/\text{CO/H}_2$ reaction.

Sulfidation of Ni/SiO_2 with H_2S lead to a blockage of bridge CO sites, a blue shift in the wavenumber of linearly adsorbed CO, an inhibition of ethylene hydrogenation, and an enhancement of the formation of propionaldehyde from ethylene hydroformylation. Isolated Ni atom sites which form linear CO may be responsible for the CO insertion leading to propionaldehyde in ethylene hydroformylation.